Supplementary Information for

Unraveling the atomic structure and dissociation of interfacial water on anatase TiO₂ (101) under ambient conditions with solid-state NMR spectroscopy†

Longxiao Yang,‡[a] Min Huang,‡[b] Ningdong Feng,*[a] Meng Wang,[c] Jun Xu,[a] Ying Jiang,[d] Ding Ma,*[c] Feng Deng*[a]

[a]State Key Laboratory of Magnetic Resonance and Atomic and Molecular Physics, National Center for Magnetic Resonance in Wuhan, Wuhan Institute of Physics and Mathematics, Innovation Academy for Precision Measurement Science and Technology, Chinese Academy of Sciences, Wuhan 430071; University of Chinese Academy of Sciences, Beijing 100049, P. R. China. ningdong.feng@wipm.ac.cn, dengf@wipm.ac.cn

[b]School of Physics, Hubei University, Wuhan 430062, P. R. China.

[c]Beijing National Laboratory for Molecular Sciences, New Cornerstone Science Laboratory, College of Chemistry and Molecular Engineering, Peking University, Beijing, China. dma@pku.edu.cn

[d]International Center for Quantum Materials, School of Physics, Peking University, Beijing, P. R. China.

†Electronic supplementary information (ESI) available.

‡These authors contributed equally to this work.

Experimental Sections

Sample Preparation. The anatase TiO_2 samples with predominantly exposed (101) facets were prepared according to previous report [1,2]. For the preparation of $Ti(OH)_4$ precursor, 6.6 mL of $TiCl_4$ was added to aqueous HCl (0.43 mol/L) drop by drop under strong stirring in an ice bath to obtain an aqueous $TiCl_4$. This aqueous $TiCl_4$ was then added to aqueous $NH_3 \cdot H_2O$ (5.5 wt.%) drop by drop under stirring. White $Ti(OH)_4$ precipitate could be formed during the process. Afterward, the aqueous $NH_3 \cdot H_2O$ (4.0 wt.%) was added to adjust the pH value to 6 − 7. After aging at room temperature for 2 h, the suspension was centrifuged, and the precipitate was washed with distilled water for three times and absolute ethanol for one time.

4.0 g the fresh $Ti(OH)_4$ precursor was first dispersed in the mixture of 30 mL deionized water and 30 ml isopropanol. After stirring and ultrasonic treatment, the suspension was transferred to a 100 mL Teflon-lined autoclave and heated for 15 h at 180 °C. The products were collected by centrifugation and washed with NaOH solution (0.1 M) and absolute ethanol for five times respectively. To remove the Cl⁻ and N attached on the surface, the product was dispersed in 200 mL NaOH solution (0.1 M) with magnetic stirring for 12 h. Finally, the white TiO_2 sample is obtained by washing with distilled water until the pH reaches 6 − 7 and drying at 60 °C for 12 h.

¹⁷O enrichment. 100 mg TiO_2 sample was enriched by 360 μmol of $H_2^{17}O$ (Cambridge Isotope Laboratories, 90%) at room temperature for 2 h, and then the ¹⁷O-enriched TiO_2 was dehydrated at 160 °C. Different amount of $H_2^{17}O$ was

introduced onto the dehydrated TiO_2 catalyst (100 mg) in a glass tube connecting to a vacuum line at the liquid N_2 temperature, and then the glass tube was sealed off. The glass tube was placed at room temperature for 2 h to equilibrate the ^{17}O enrichment process. Prior to the NMR experiments, the ^{17}O enriched samples with or without loaded $H_2^{17}O$ were transferred into a NMR rotor in the glove box.

^2H enrichment. The dehydrated ^2H-enriched TiO_2 (100 mg) was prepared by exchanging TiO_2 with 470 μmol of ^2H_2O (Sigma-Aldrich, 99.9%) at room temperature for 2 h, and then the ^2H-enriched sample was dehydrated at 160 °C. The dehydrated ^2H-enriched TiO_2 was then loaded with different amount (0.3 − 4.7 mmol/g) of ^2H_2O.

Characterization. X-ray diffraction patterns (XRD) of the samples were acquired on a X´PERT^3 POWDER with Cu radiation (λ = 0.15418 nm). The morphology of TiO_2 was characterized by transmission electron microscopy (TEM) on a Tecnai F30 at an accelerating voltage of 300 KV. Nitrogen adsorption/desorption isotherm measurements were conducted at an ASAP 2460 for the BET area. X-ray photoelectron spectroscopy (Thermo Escalab 250Xi, Al Ka irradiation, XPS) was adopted to detect the residue of Cl^-, N impurities on the TiO_2 surface. The C 1s peak (284.6 eV) arising from adventitious carbon was chosen as the reference of the binding energy.

^{17}O MAS NMR experiments were conducted at 11.7 T (^{17}O Larmor frequency of 67.8MHz) on a Bruker-Advance III 500 spectrometer using a 4 mm double-resonance probe. The 1D ^{17}O MAS NMR spectra were recorded by using a π/12 pulse width of 0.3 μs, a repetition time of 0.5 s, a magic angle spinning

rate of 13.5 kHz, and 600000 scans accumulations. 2D ^{17}O 3Q MAS NMR experiments were carried out using Z-fliter sequence with a pulse delay of 0.5 s and a magic angle spinning rate of 13.5 kHz. The increment interval in the indirect dimension was set to 52.59 μs, and 32 t_1 increments and 36000 scans accumulations for each t_1 increment were used in the NMR experiments. The total time for acquiring a 1D ^{17}O MAS spectrum is ca. three-four days and that for acquiring a 2D ^{17}O 3Q MAS NMR spectrum is up to six days. 2D ^{1}H{^{17}O} J-HMQC spectra were collected at a magic angle spinning speed of 13.5 kHz with a recycle delay of 1.5 s. The increment interval in the indirect dimension was set to 74.07 μs, and 80 t_1 increments were used in the NMR experiments. A total of 128, 512, 128 scans were collected respectively for the 2D ^{1}H{^{17}O} J-HMQC spectra in the ^{17}O chemical shift range of -50 − 40, 110 − 190, 590 − 710 ppm. The total time for acquiring a 2D ^{1}H{^{17}O} J-HMQC spectrum is 4 − 16 hours.

The 1D ^{17}O MAS NMR spectra were also recorded at 18.8 T (^{17}O Larmor frequency of 108.5 MHz) on a Bruker-Advance III 800 spectrometer using a 1.9 mm double-resonance probe. A π/2 pulse width of 2.5 μs and a repetition time of 1 s were used to collect the 1D ^{17}O MAS NMR spectra at a spinning speed of 35 kHz.

Variable-temperature static ^{2}H NMR experiments were performed on a Bruker Avance III 400 MHz DNP spectrometer and a double-resonance 1.9 mm probe. A solid echo pulse sequence [π/2 - τ - π/2- τ - acquire] was used to acquire static ^{2}H NMR spectra, in which echo delay, π/2 pulse length and recycle

delay were 30 μs, 2.9 μs and 2 s, respectively. Deconvolution of the ^{2}H NMR spectra was conducted using DMFIT software.

^{2}H MAS NMR experiments were performed on a Bruker-Advance III 500 spectrometer with a double-resonance 4.0 mm probe. A π/2 pulse width of 5 μs and a recycle delay of 4 s were used to collect the 1D ^{2}H MAS NMR spectra at a spinning speed of 10 kHz.

Theoretical calculations. Density functional theory (DFT) calculations were performed by using Vienna Ab initio Simulation Package (VASP) computer package with the Perdew-Burke-Ernzerhof (PBE) generalized gradient corrected approximation (GGA) for the exchange-correlation function [3,4]. Projector-augmented wave (PAW) potentials were used to take into account the electron-ion interaction, and the wave function was described with a plane wave basis set of 500 eV. Similar to previous study which showed standard DFT can give reliable structural information, we used standard DFT method to do all the calculations [5]. To make our calculation results more reliable, we used the experimental values (a = 3.78 Å and c = 9.50 Å) for the lattice constant of bulk anatase TiO_2 in our calculations [6]. The anatase TiO_2 (101) surfaces were modeled by (2×2) surface slabs with 24 atomic layers and vacuum thickness of 15 Å to maintain trivial fluctuations of chemical shift values in their middle layers. The chemical shifts of O were calculated by using the linear response method. The k-point meshes employed in the calculations were generated according to the Monkhorst-Pack scheme [7]. The resulting Brillouin-zone sampling used for the supercells was equivalent to the one obtained with (4×4×1) grids for the primitive

(1×1) slabs of the surface. Spin polarization was included in the calculations. All of the atoms were allowed to relax during structure optimization until the change of the total energy was less than 1×10^{-5} eV and all the forces on each atom were smaller than 0.01 eV/Å.

The isotropic chemical shift (δ) can be computed as $\delta = \delta_{cal} + \delta_{ref}$ where δ_{cal} is the chemical shift calculated by VASP, δ_{ref} is the reference chemical shift. The δ_{ref} for each model was determined by aligning the average δ_{cal} of middle four layers to the experimental δ_{iso} of bulk O_{3C} (561 ppm).
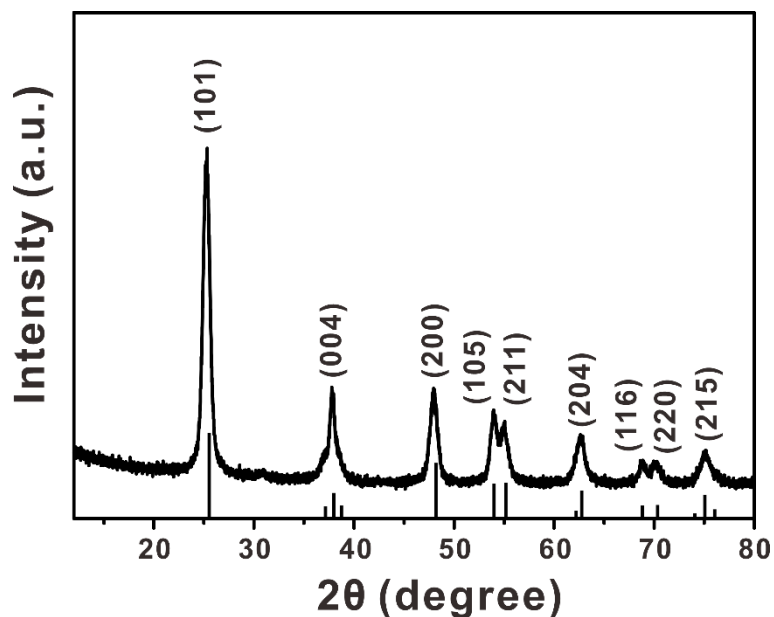
Figure S1. XRD patterns and standard PDF card of the anatase TiO_2 sample.
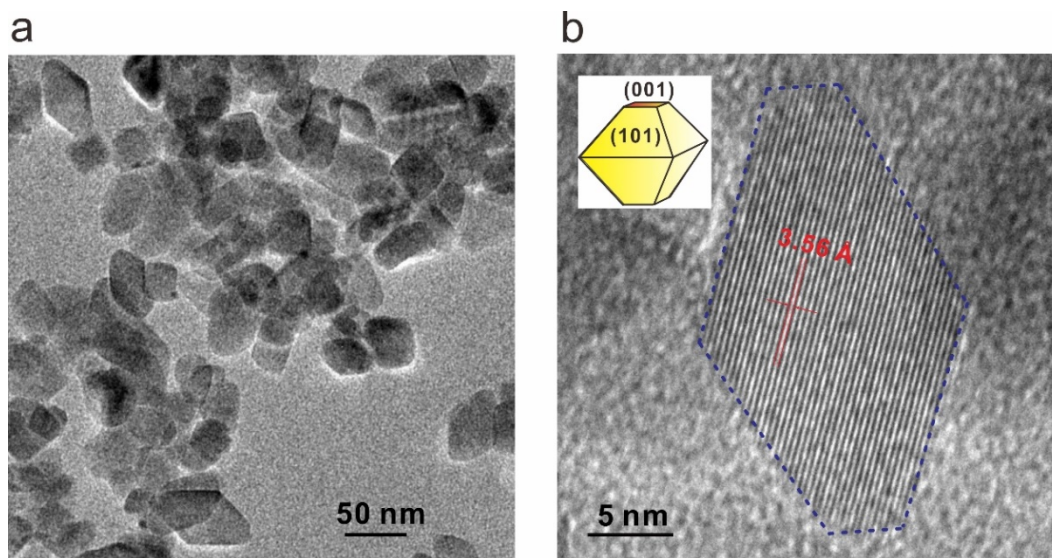

Figure S2. (a) Low magnification and (b) high resolution TEM images of the TiO_2 sample. Inset in b shows the schematic diagram of the TiO_2 nanoparticle. The TEM results indicate that the TiO_2 sample exhibits an octahedral morphology with an average size of 20 nm. The lattice spacing parallel to the lateral facets is 3.56 Å, corresponding to the (101) facet of anatase TiO_2, and the percentage of the dominant facet is about 95%, which is the most frequently exposed surface with the lowest energy [8,9].
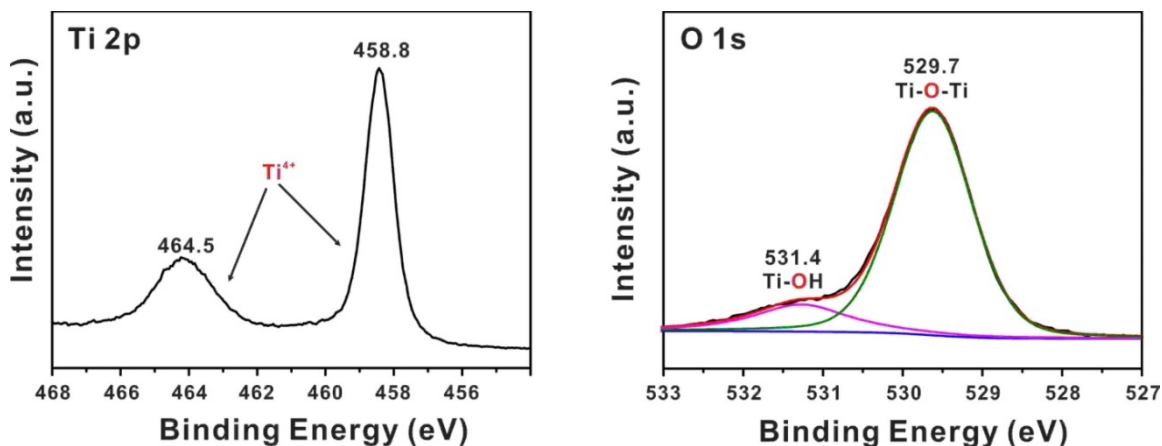
Figure S3. Ti *2p*, and O *1s* XPS spectra of the TiO_2 sample. According to the XPS results, titanium atoms exist in the form of $Ti^{4+}-O$ bonds as confirmed by the Ti $2p_{3/2}$ and $2p_{1/2}$ XPS peaks at 458.8 and 464.5 eV, and the O *1s* XPS spectra shows two peaks at 529.7 and 531.4 eV, due to lattice oxygen in Ti−O−Ti bonds and OH groups, respectively[10].
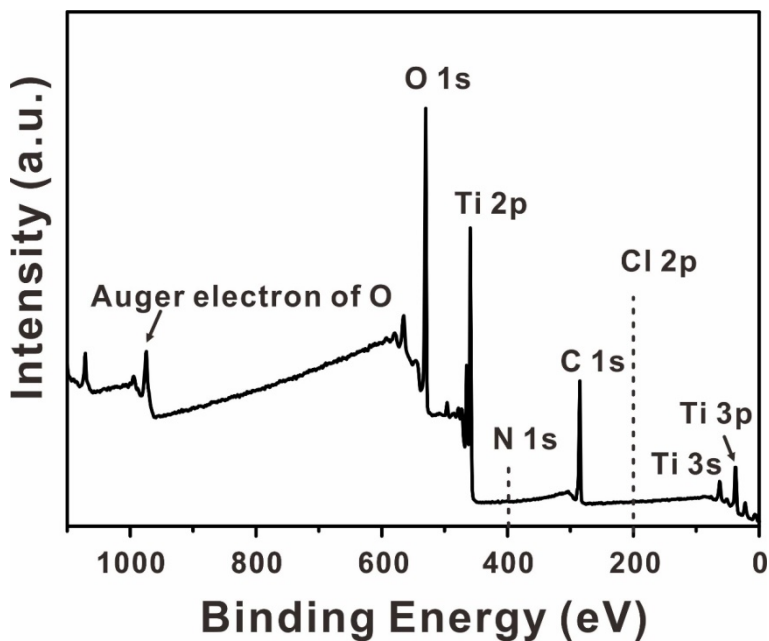

Figure S4. XPS patterns of the TiO_2 sample. Cl^- (200 eV) and N (400 eV) species are not observed on the surface, indicating the absence of chlorine and nitrogen species on the TiO_2 surface.
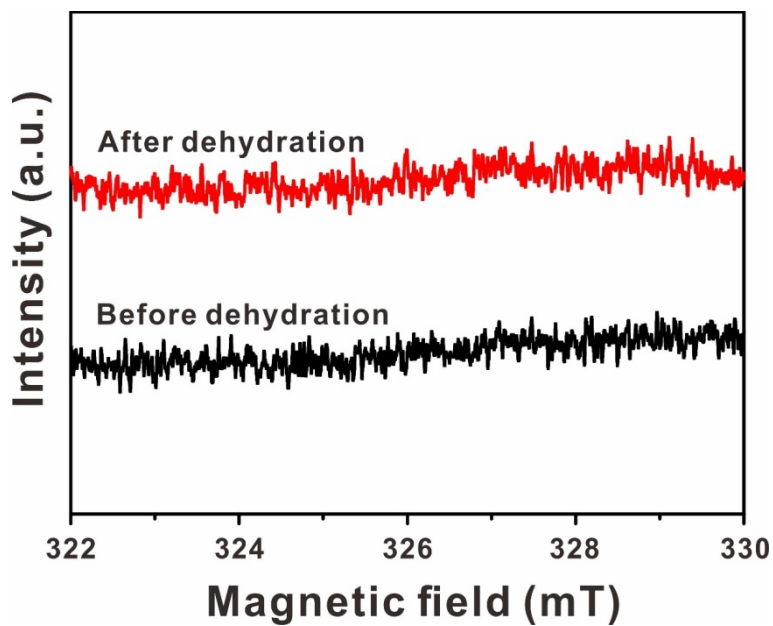
Figure S5. ESR spectra (acquired at liquid nitrogen temperature) of the TiO$_2$ sample before and after dehydration at 160 °C.
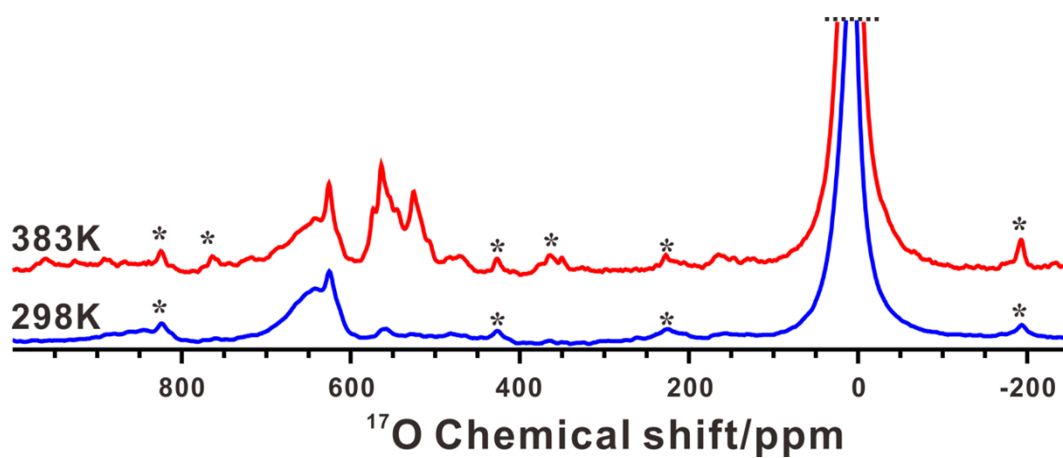
Figure S6. 1D ^{17}O MAS NMR spectra of dehydrated ^{17}O-enriched TiO$_2$ loaded with 3.1 mmol/g H$_2$^{17}O at 298 K and 383 K, acquired at magnetic field of 11.7 T.

Figure S7. 2D ^{17}O 3Q MAS NMR spectrum of dehydrated ^{17}O-enriched TiO_2 with 0.3 mmol/g $H_2{}^{17}O$ loading, acquired at magnetic field of 11.7 T.
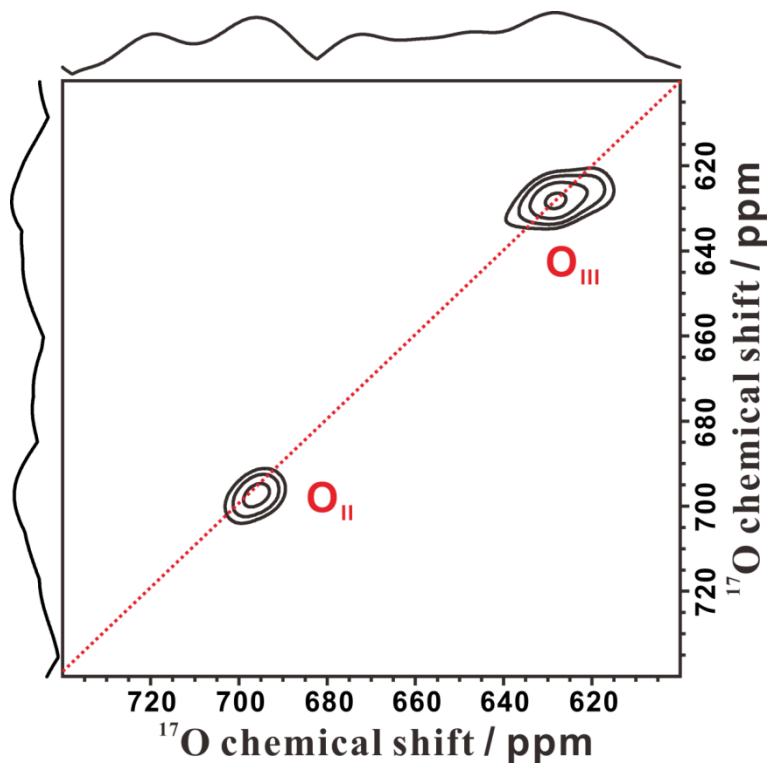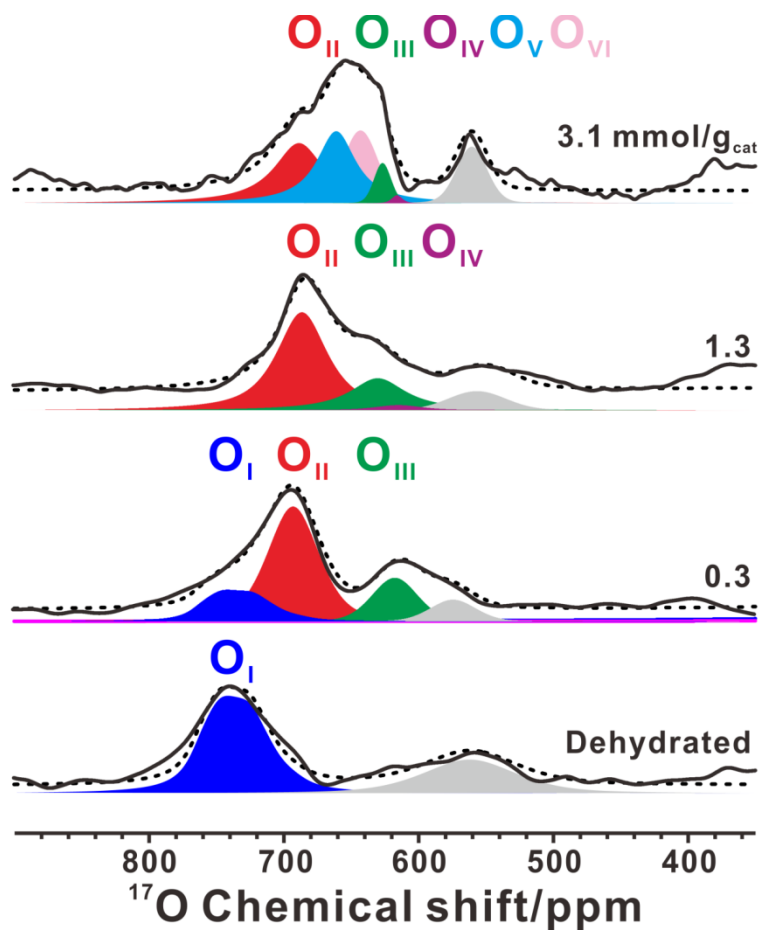
Figure S8. 1D ^{17}O MAS NMR spectra of dehydrated ^{17}O-enriched TiO_2 samples with $H_2^{17}O$ loading from 0 to 3.1 mmol/g, acquired at magnetic field of 18.7 T. The signal (gray) at 500 − 600 ppm is due to the bulk oxygen species.
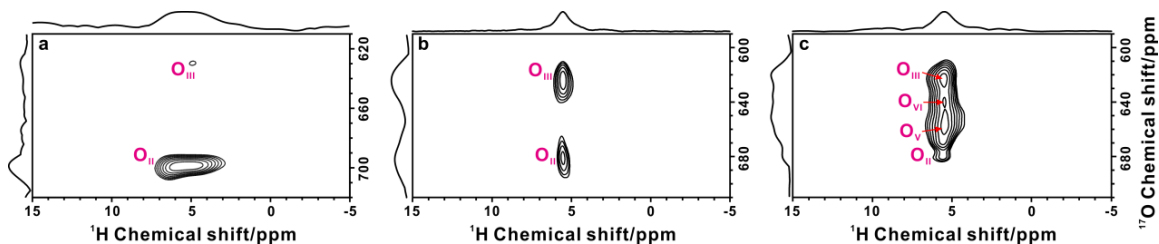
Figure S9. 2D ^{1}H{^{17}O} J-HMQC NMR spectra of dehydrated ^{17}O-enriched TiO$_2$ samples with (a) 0.5, (b) 1.3 and (c) 3.1 mmol/g H$_2$^{17}O loading. When the H$_2$^{17}O loading is 0.5 mmol/g, two correlations are visible between the ^{1}H signal (at 5.4 ppm) of molecular H$_2$O and the ^{17}O signals of O$_{II}$ (at 700 ppm) and O$_{III}$ (at 628 ppm) sites (Figure S9a). When the H$_2$^{17}O loading is 1.3 mmol/g, the ^{1}H signal (at 5.4 ppm) of molecular H$_2$O also interacts with the two types of surface O$_{2C}$ sites (that is O$_{II}$ and O$_{III}$, Figure S9b). With the increase of H$_2$O loading to 3.1 mmol/g, four correlations are evident between the ^{1}H signal (at 5.4 ppm) of molecular H$_2$O and the ^{17}O signals of O$_{II}$ (at 678 ppm), O$_{III}$ (at 628 ppm), O$_V$ (at 658 ppm), and O$_{VI}$ (at 640 ppm) sites (Figure S9c). Note that there is no correlation observed between these O$_{2C}$ sites and surface OH groups. Thus, the formation of O$_{II}$ − O$_{VI}$ sites is only associated with interaction between O$_I$ (the bare O$_{2c}$ site) and molecular H$_2$O, and has nothing to do with surface OH groups. Additionally, the correlation signal between the ^{1}H signal (at 5.4 ppm) of adsorbed H$_2$O and the ^{17}O signal (at 615 ppm) of O$_{IV}$ is not observable, probably due to its low amount and high mobility.
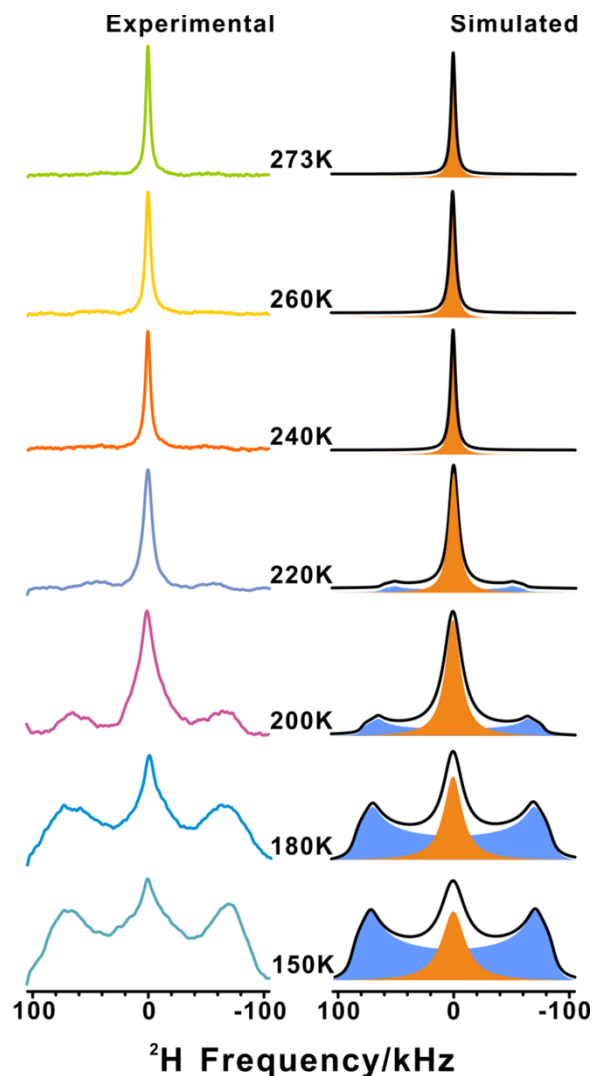
Figure S10. Experimental (left) and simulated (right) static ^{2}H NMR spectra of TiO_2 with 1.3 mmol/g D_2O loading, acquired at variable temperature. Two peaks with different lineshape are evident at low temperature (150 − 220 K), confirming the existence of two types of adsorbed D_2O (that is chemisorbed and physisorbed D_2O). According to the 2D ^{1}H{^{17}O} J-HMQC NMR experiments, the chemisorbed D_2O not only interacts with two types of surface hydroxyl groups (Figure 2 in main text) and O_{2C} sites (Figure S9), but also bonds to Ti_{5C} site (D_2O-Ti_{5c}) on the TiO_2 surface, forming a relatively rigid structure. The peak of the chemisorbed D_2O shows a broad ^{2}H quadrupolar pattern at 150 K, and its NMR parameters (δ_{iso}, C_Q, and η) are listed in Table S4. While the physisorbed D_2O only interacts with the chemisorbed D_2O and terminal hydroxyl group, and has relatively high mobility, leading to a narrow peak with Gaussian lineshape. When the temperature increases from 150 K to 220 K, the ^{2}H quadrupolar pattern gradually disappears, which can be ascribed to the fast exchange between chemisorbed and physisorbed D_2O molecules.
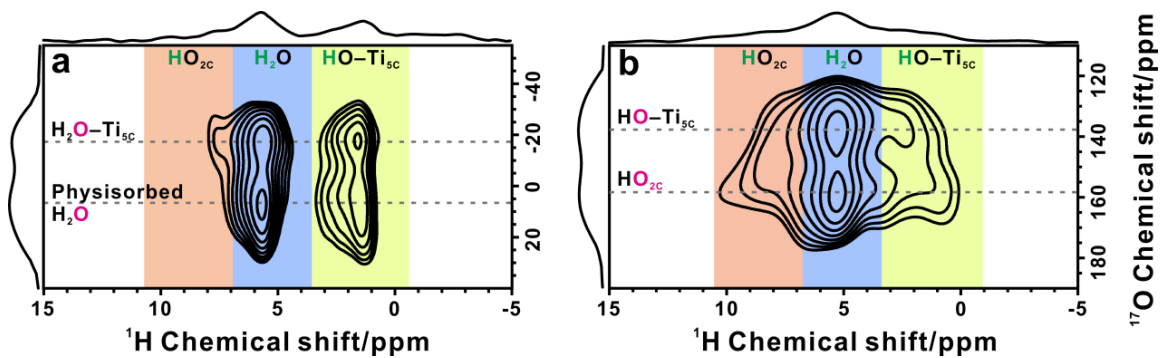
Figure S11. 2D $^1H\{^{17}O\}$ J-HMQC NMR spectra (a, b) of dehydrated ^{17}O-enriched TiO_2 with 1.3 mmol/g $H_2^{17}O$ loading in different ^{17}O chemical shift range.

Bare TiO₂

Layer of O	δ_{iso}/ppm
1	798
2	492
3	521
4	559
5	559
6	538
7	555
8	558
9	561
10	552
11	555
12	561
13	560
14	555
15	552
16	559
17	559
18	555
19	538
20	559
21	558
22	522
23	493
24	800

Figure S12. Calculated structure of the bare TiO₂ (101) facet. Isotropic chemical shifts δ_{iso} of the oxygen sites in each layer are listed, for which δ_{ref} = 133. Titanium and oxygen atoms are plotted in blue (Ti) and red (O).

1 H₂O/1 Ti₅c

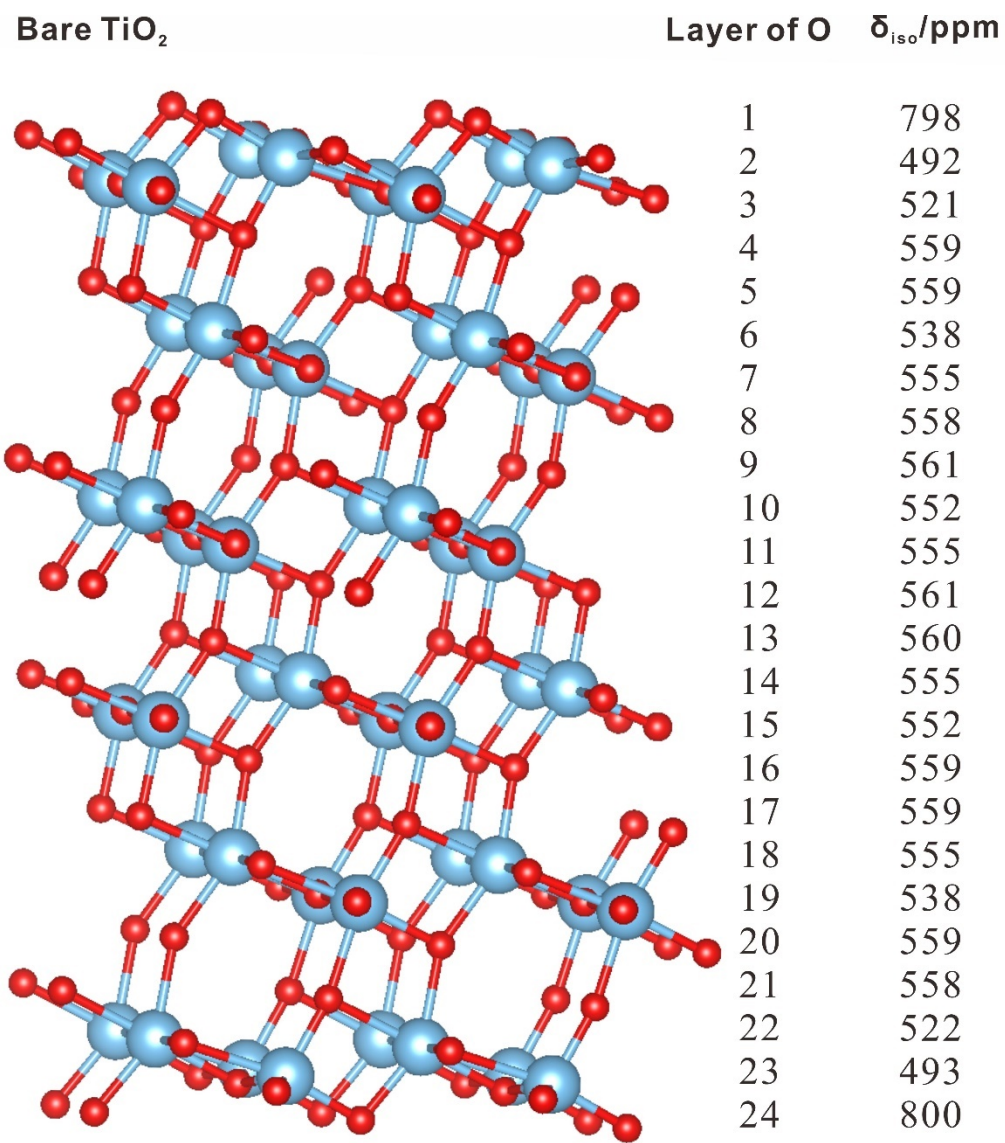| Layer of O	δ_{iso}/ppm
H₂O	-32
1	725, 723, 794, 793
2	494, 491, 494, 494
3	533, 532, 550, 541
4	549, 550, 573, 550
5	560, 569, 548, 546
6	533, 534, 551, 551
7	552, 552, 558, 561
8	554, 554, 565, 559
9	563, 563, 563, 563
10	555, 555, 555, 555
11	554, 554, 554, 554
12	561, 561, 561, 561
13	558, 558, 558, 558
14	557, 557, 557, 557
15	551, 551, 551, 551
16	558, 558, 558, 558
17	555, 555, 555, 555
18	555, 555, 555, 555
19	562, 562, 562, 562
20	551, 552, 533, 570
21	552, 574, 549, 550
22	536, 549, 533, 532
23	494, 495, 534, 491
24	794, 795, 721, 724
H₂O	-32

Figure S13. Calculated structure of the TiO_2 (101) facet with adsorbed water molecules. In this model, one water molecule is chemisorbed on one surface Ti_{5C} site. This structure is denoted as $1H_2O/1Ti_{5C}$ in the text. Isotropic chemical shifts δ_{iso} of the oxygen sites in each layer are listed, for which δ_{ref} = 135. Titanium, oxygen and hydrogen atoms are plotted in blue (Ti), red (O) and pink (H).

2H$_2$O/2Ti$_{5C}$

Layer of O	δ_{iso}/ppm
H$_2$O	-36
1	729, 727
2	499, 498
3	555, 542
4	569, 550
5	546, 555
6	547, 545
7	556. 556
8	561, 561
9	559, 559
10	556, 556
11	556, 556
12	561, 561
13	557. 557
14	555, 555
15	553, 553
16	558, 558
17	552, 552
18	559, 556
19	547, 547
20	546, 554
21	550, 570
22	543, 557
23	500, 500
24	724, 726
H$_2$O	-37

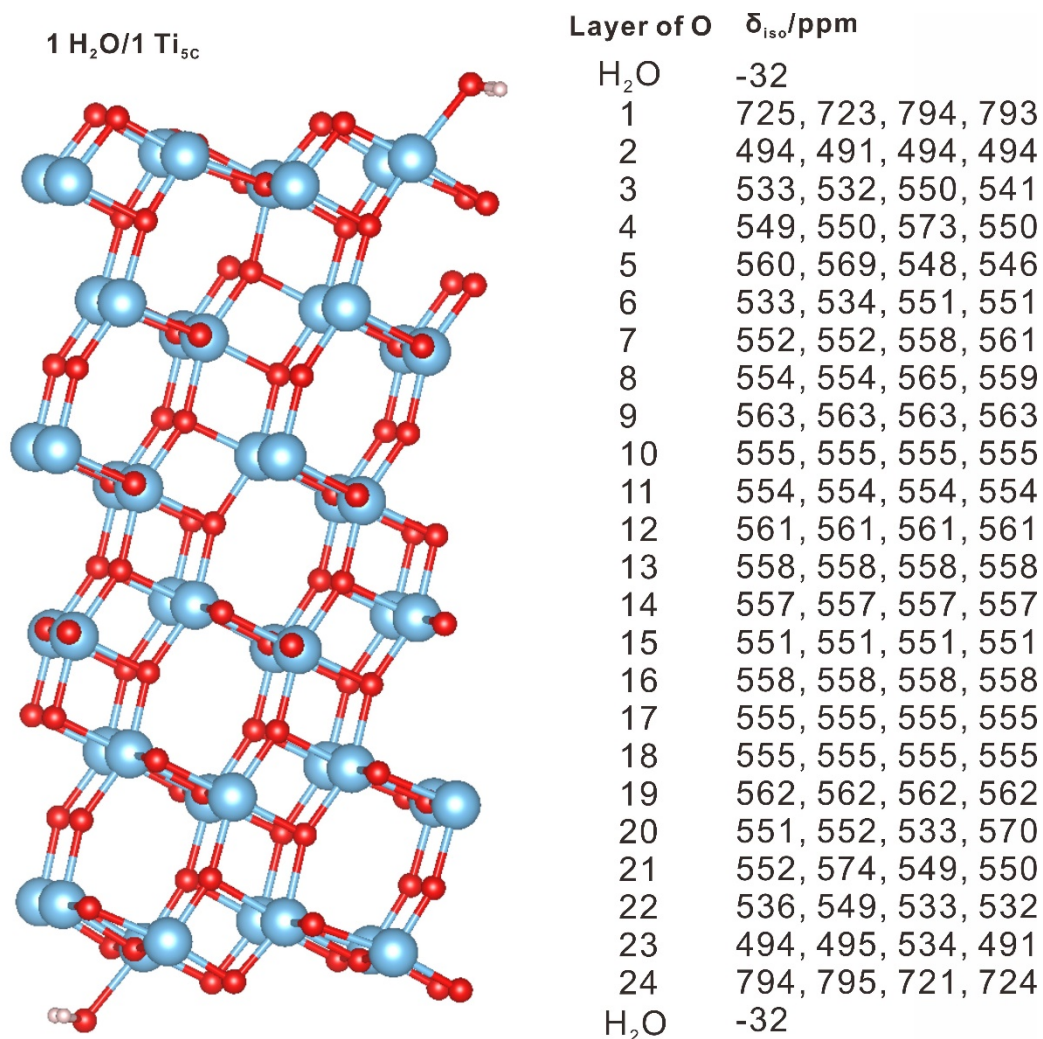**Figure S14.** Calculated structure of the TiO$_2$ (101) facet with adsorbed water molecules. In this model, two water molecules are chemisorbed on two surface Ti$_{5C}$ site. This structure is denoted as 2H$_2$O/2Ti$_{5C}$ in the text. Isotropic chemical shifts δ_{iso} of the oxygen sites in each layer are listed, for which δ_{ref} = 135. Titanium, oxygen and hydrogen atoms are plotted in blue (Ti), red (O) and pink (H).
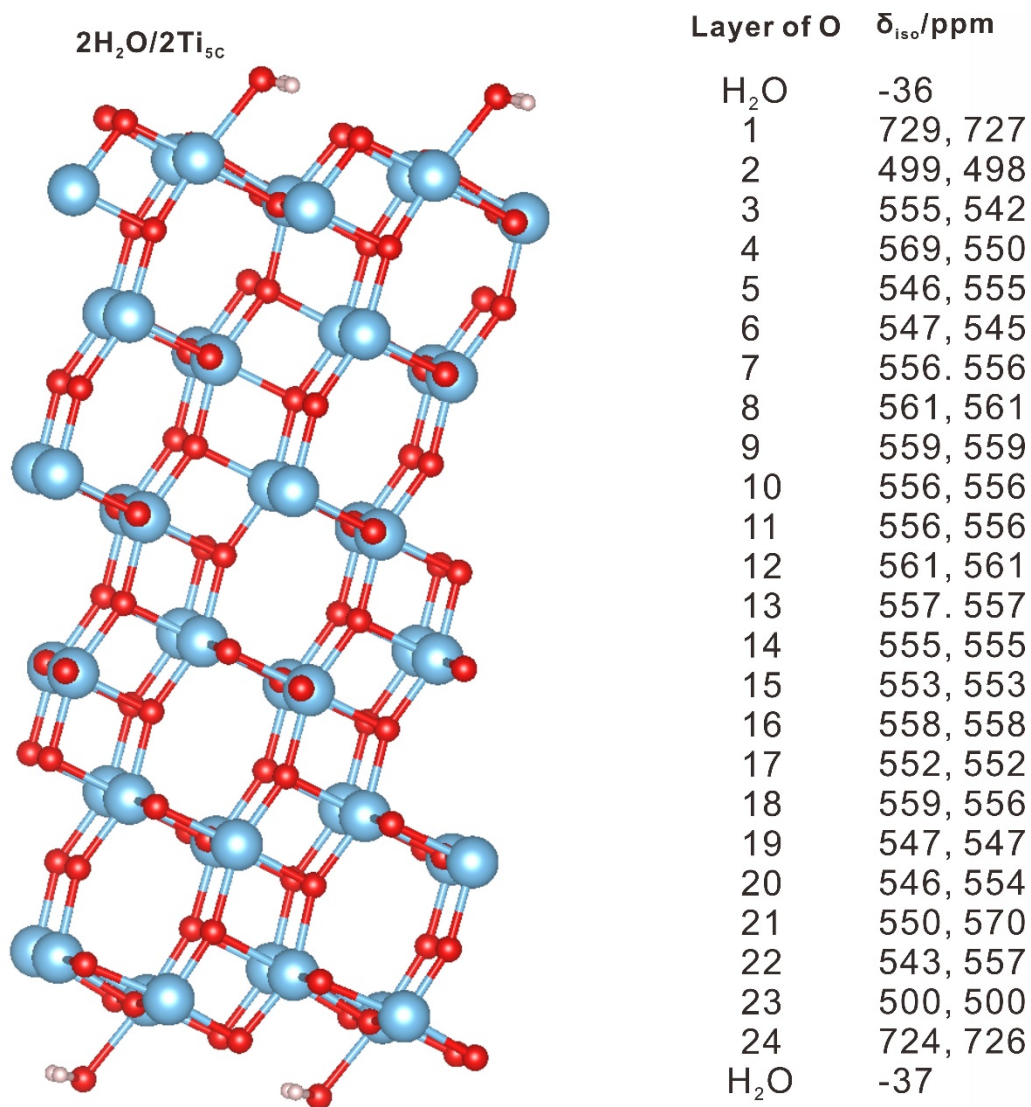
17

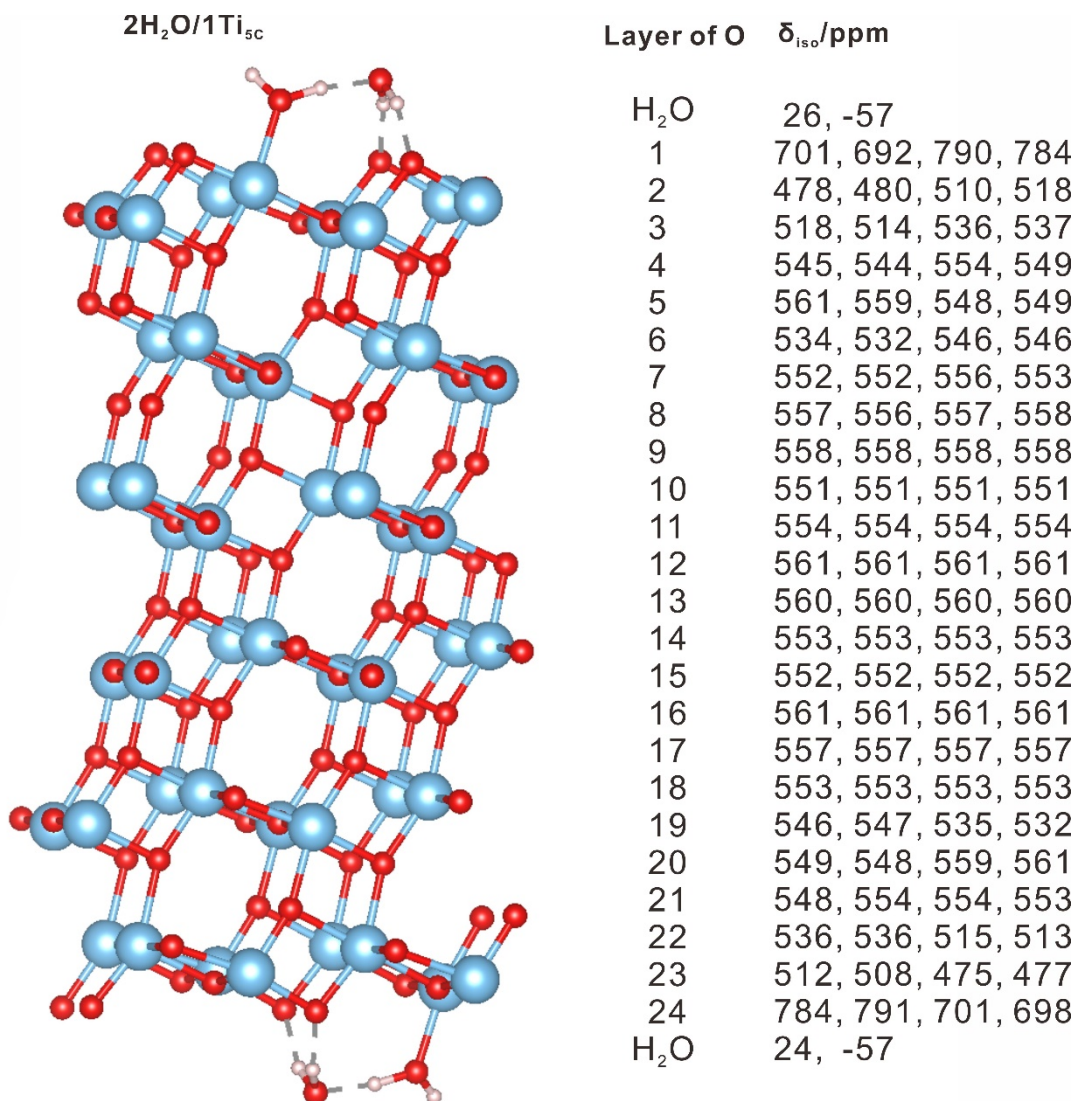| 2H$_2$O/1Ti$_{5C}$	Layer of O	δ_{iso}/ppm
	H$_2$O	26, -57
	1	701, 692, 790, 784
	2	478, 480, 510, 518
	3	518, 514, 536, 537
	4	545, 544, 554, 549
	5	561, 559, 548, 549
	6	534, 532, 546, 546
	7	552, 552, 556, 553
	8	557, 556, 557, 558
	9	558, 558, 558, 558
	10	551, 551, 551, 551
	11	554, 554, 554, 554
	12	561, 561, 561, 561
	13	560, 560, 560, 560
	14	553, 553, 553, 553
	15	552, 552, 552, 552
	16	561, 561, 561, 561
	17	557, 557, 557, 557
	18	553, 553, 553, 553
	19	546, 547, 535, 532
	20	549, 548, 559, 561
	21	548, 554, 554, 553
	22	536, 536, 515, 513
	23	512, 508, 475, 477
	24	784, 791, 701, 698
	H$_2$O	24, -57

Figure S15. Calculated structure of the TiO$_2$ (101) facet with adsorbed water molecules. In this model, one water molecule is chemisorbed on one surface Ti$_{5C}$ site and another water molecule is physisorbed on the H$_2$O−Ti$_{5C}$ through hydrogen bond. This structure is denoted as 2H$_2$O/1Ti$_{5C}$ in the text. Isotropic chemical shifts δ_{iso} of the oxygen sites in each layer are listed, for which δ_{ref} = 133. Titanium, oxygen and hydrogen atoms are plotted in blue (Ti), red (O) and pink (H).
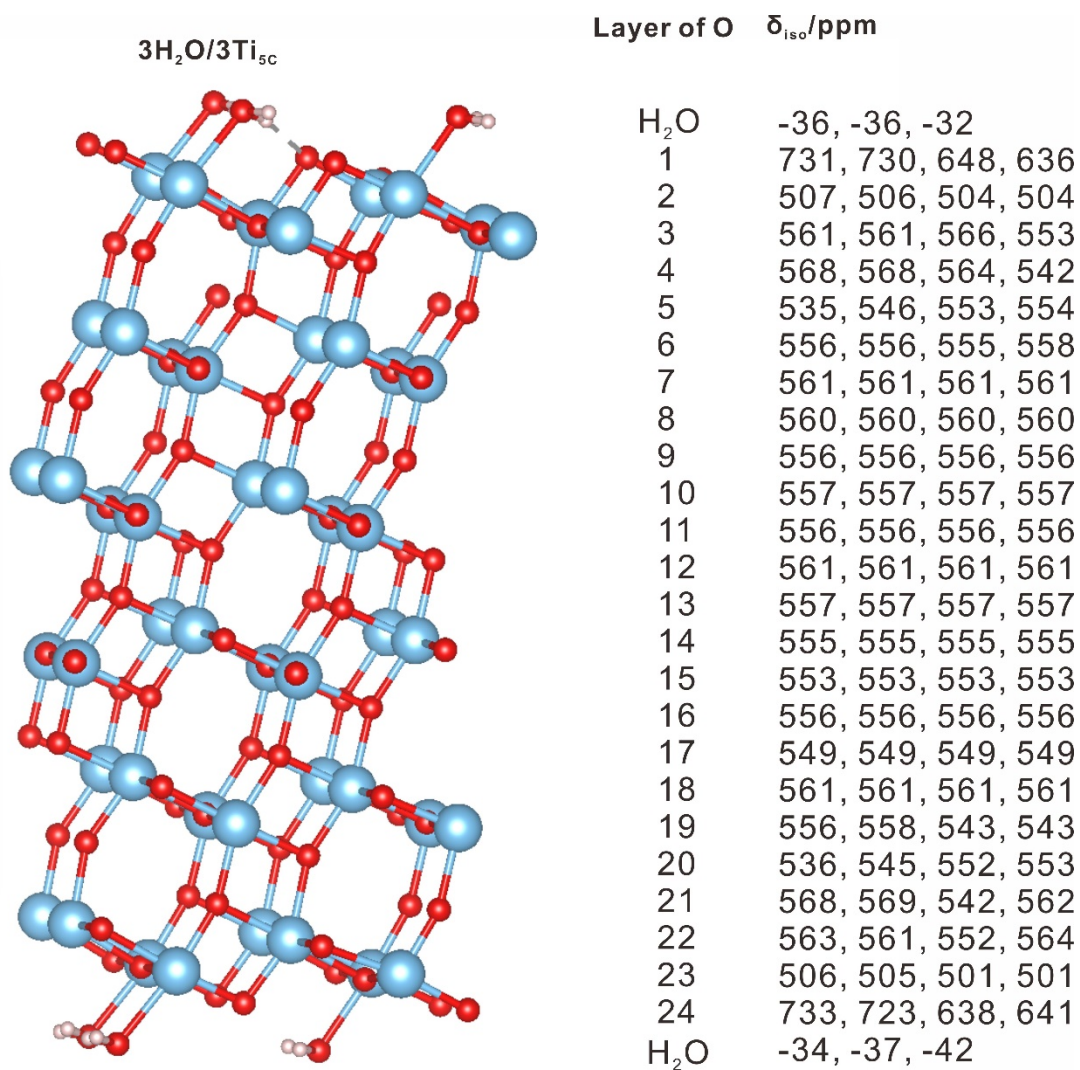
3H$_2$O/3Ti$_{5C}$

Layer of O	δ_{iso}/ppm
H$_2$O	-36, -36, -32
1	731, 730, 648, 636
2	507, 506, 504, 504
3	561, 561, 566, 553
4	568, 568, 564, 542
5	535, 546, 553, 554
6	556, 556, 555, 558
7	561, 561, 561, 561
8	560, 560, 560, 560
9	556, 556, 556, 556
10	557, 557, 557, 557
11	556, 556, 556, 556
12	561, 561, 561, 561
13	557, 557, 557, 557
14	555, 555, 555, 555
15	553, 553, 553, 553
16	556, 556, 556, 556
17	549, 549, 549, 549
18	561, 561, 561, 561
19	556, 558, 543, 543
20	536, 545, 552, 553
21	568, 569, 542, 562
22	563, 561, 552, 564
23	506, 505, 501, 501
24	733, 723, 638, 641
H$_2$O	-34, -37, -42

Figure S16. Calculated structure of the TiO$_2$ (101) facet with adsorbed water molecules. In this model, three water molecules are chemisorbed on three surface Ti$_{5C}$ sites. This structure is denoted as 3H$_2$O/3Ti$_{5C}$ in the text. Isotropic chemical shifts δ_{iso} of the oxygen sites in each layer are listed, for which δ_{ref} = 133. Titanium, oxygen and hydrogen atoms are plotted in blue (Ti), red (O) and pink (H).
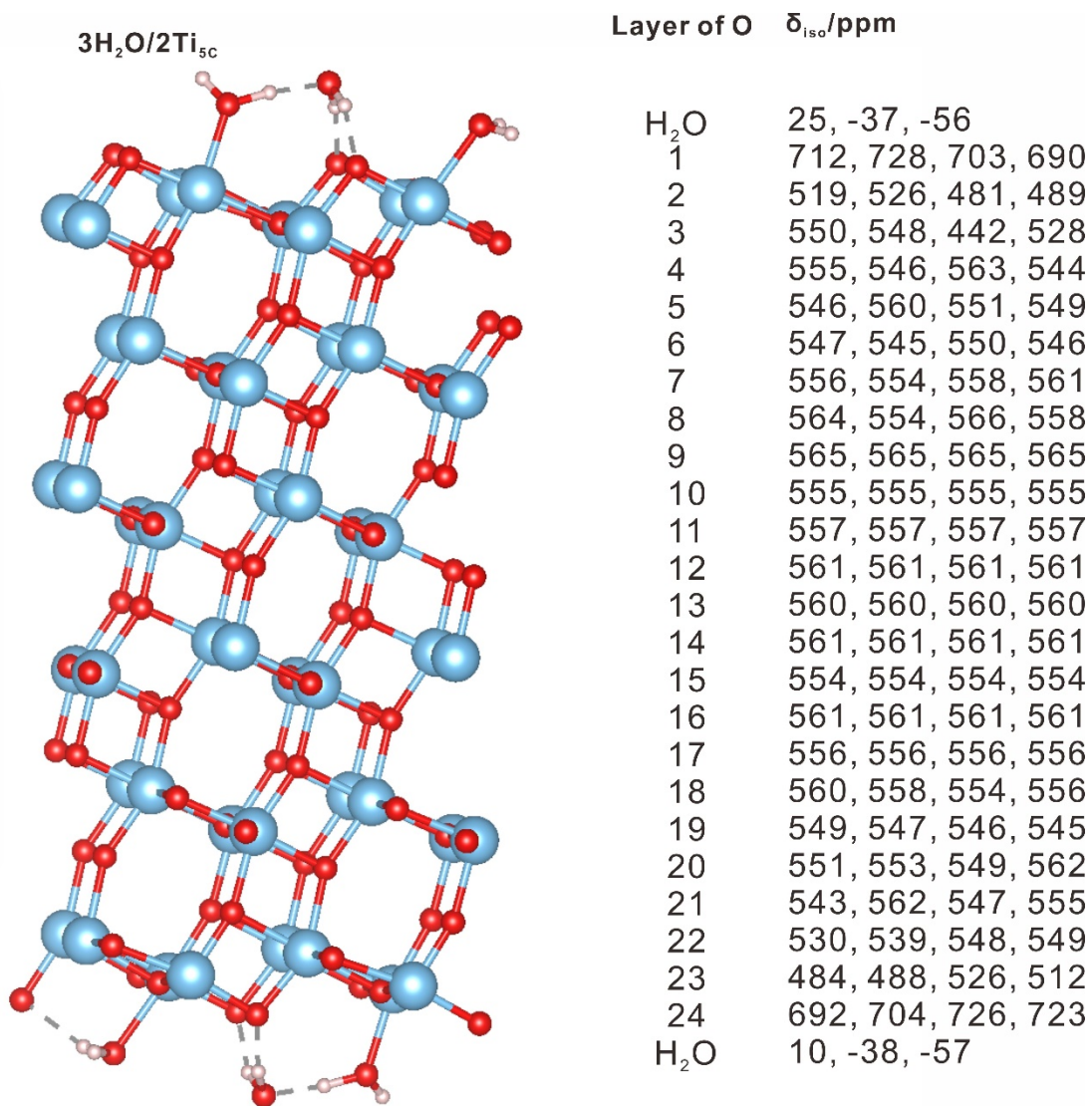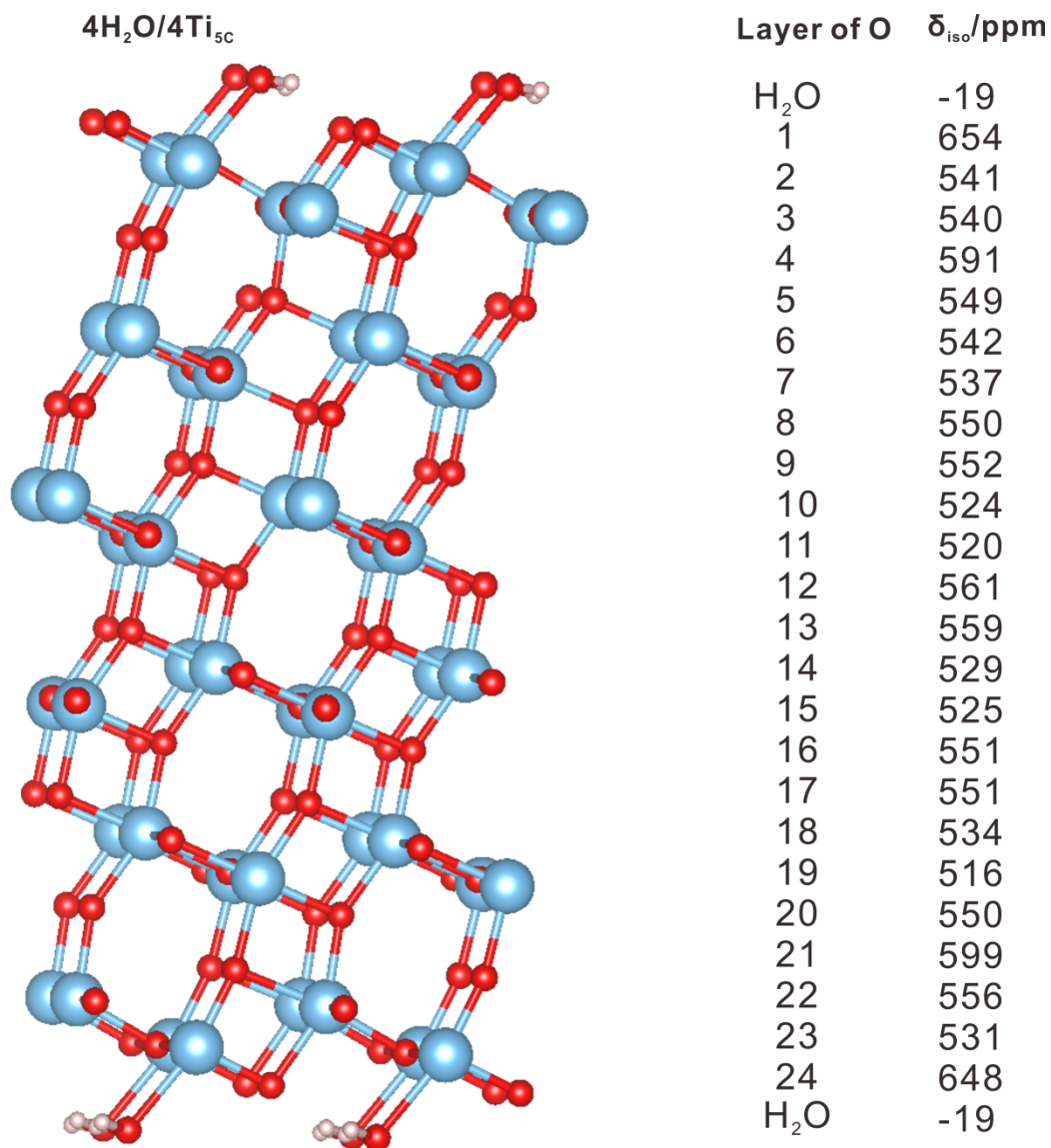
Layer of O	δ_{iso}/ppm
H_2O	25, -37, -56
1	712, 728, 703, 690
2	519, 526, 481, 489
3	550, 548, 442, 528
4	555, 546, 563, 544
5	546, 560, 551, 549
6	547, 545, 550, 546
7	556, 554, 558, 561
8	564, 554, 566, 558
9	565, 565, 565, 565
10	555, 555, 555, 555
11	557, 557, 557, 557
12	561, 561, 561, 561
13	560, 560, 560, 560
14	561, 561, 561, 561
15	554, 554, 554, 554
16	561, 561, 561, 561
17	556, 556, 556, 556
18	560, 558, 554, 556
19	549, 547, 546, 545
20	551, 553, 549, 562
21	543, 562, 547, 555
22	530, 539, 548, 549
23	484, 488, 526, 512
24	692, 704, 726, 723
H_2O	10, -38, -57

Figure S17. Calculated structure of the TiO_2 (101) facet with adsorbed water molecules. In this model, two water molecules are chemisorbed on two surface Ti_{5C} site and another one water molecule is physisorbed on the H_2O-Ti_{5C} through hydrogen bond. This structure is denoted as $3H_2O/2Ti_{5C}$ in the text. Isotropic chemical shifts δ_{iso} of the oxygen sites in each layer are listed, for which δ_{ref} = 135. Titanium, oxygen and hydrogen atoms are plotted in blue (Ti), red (O) and pink (H).
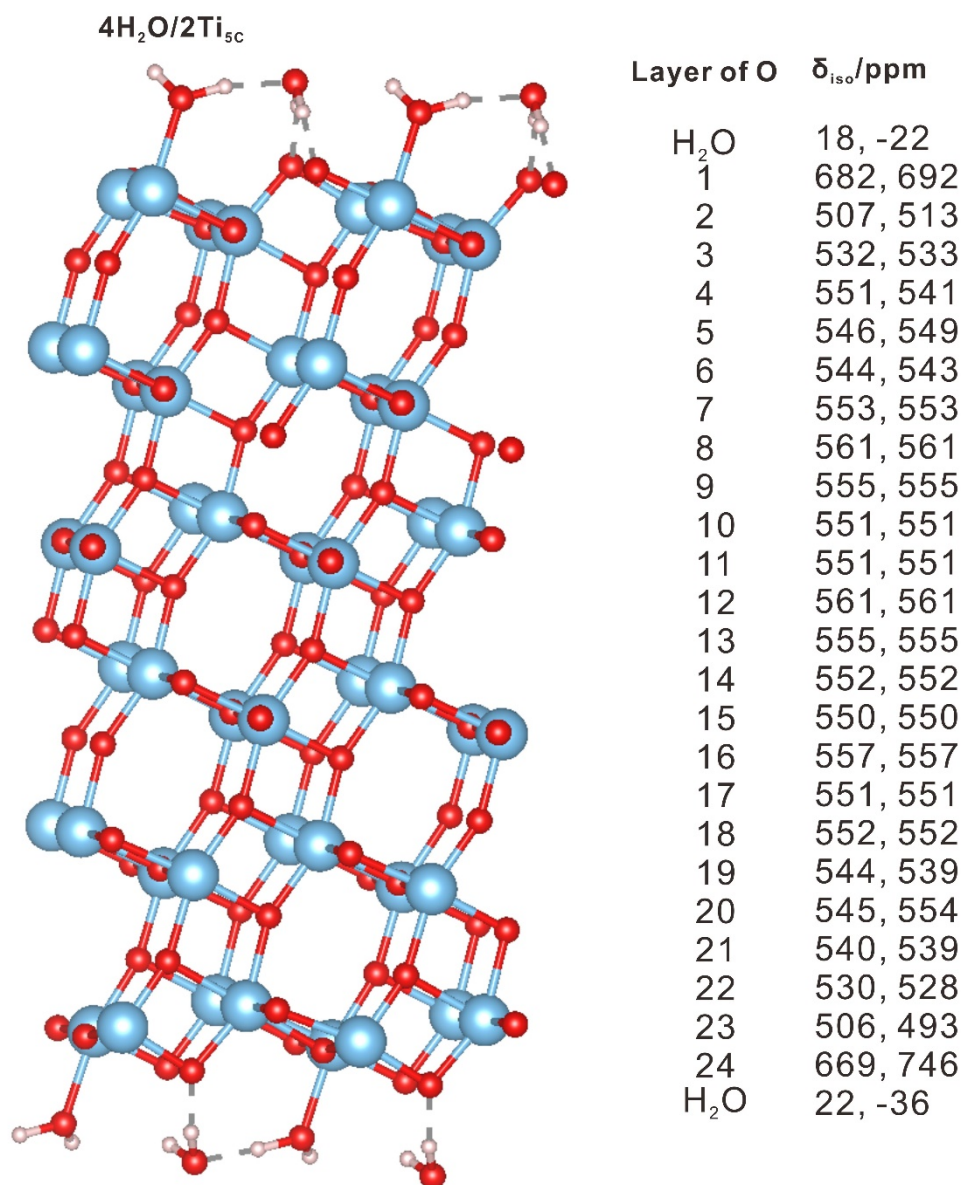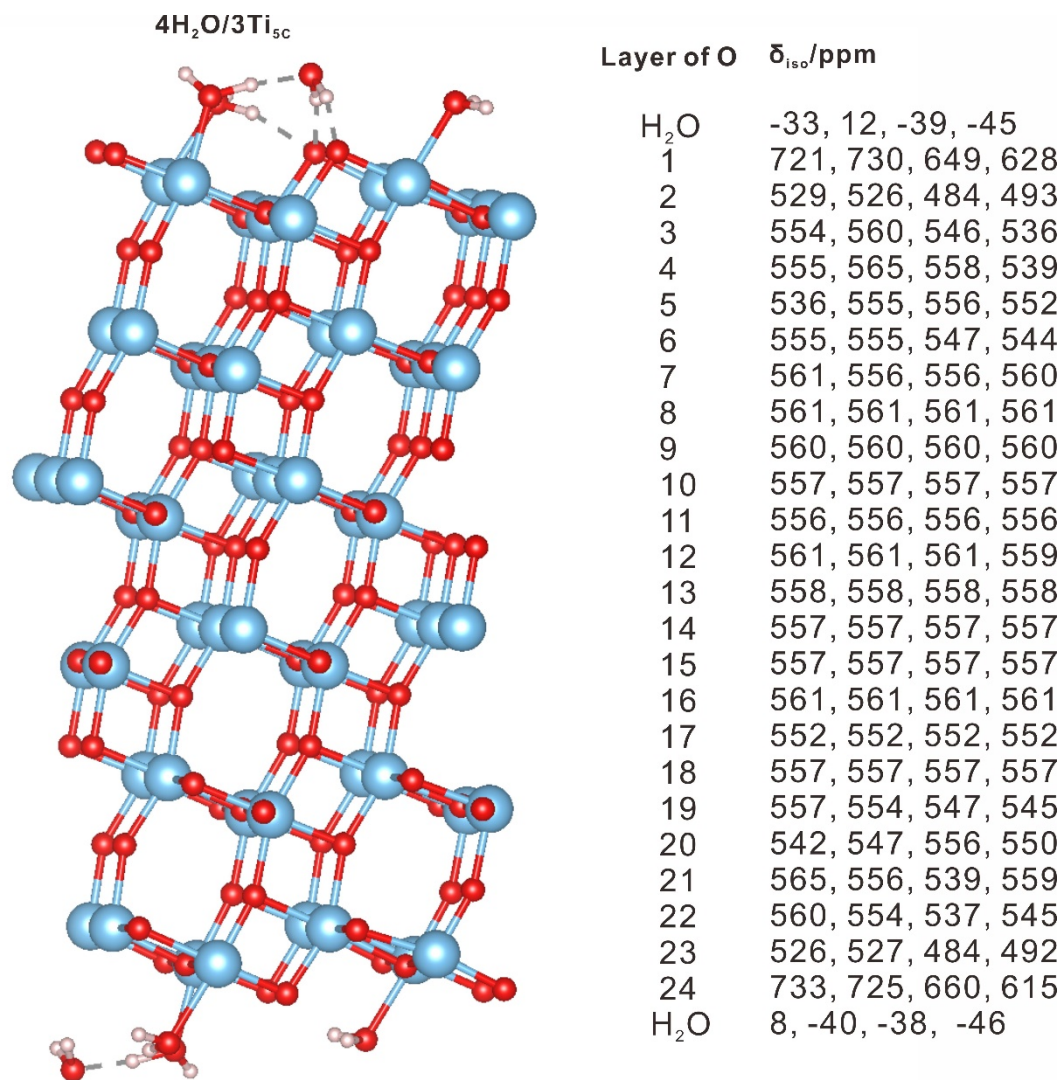
4H₂O/4Ti₅C

Layer of O	δ_{iso}/ppm
H₂O	-19
1	654
2	541
3	540
4	591
5	549
6	542
7	537
8	550
9	552
10	524
11	520
12	561
13	559
14	529
15	525
16	551
17	551
18	534
19	516
20	550
21	599
22	556
23	531
24	648
H₂O	-19

Figure S18. Calculated structure of the TiO_2 (101) facet with adsorbed water molecules. In this model, four water molecules are chemisorbed on four surface Ti_{5C} sites. This structure is denoted as $4H_2O/4Ti_{5C}$ in the text. Isotropic chemical shifts δ_{iso} of the oxygen sites in each layer are listed, for which δ_{ref} = 132. Titanium, oxygen and hydrogen atoms are plotted in blue (Ti), red (O) and pink (H).
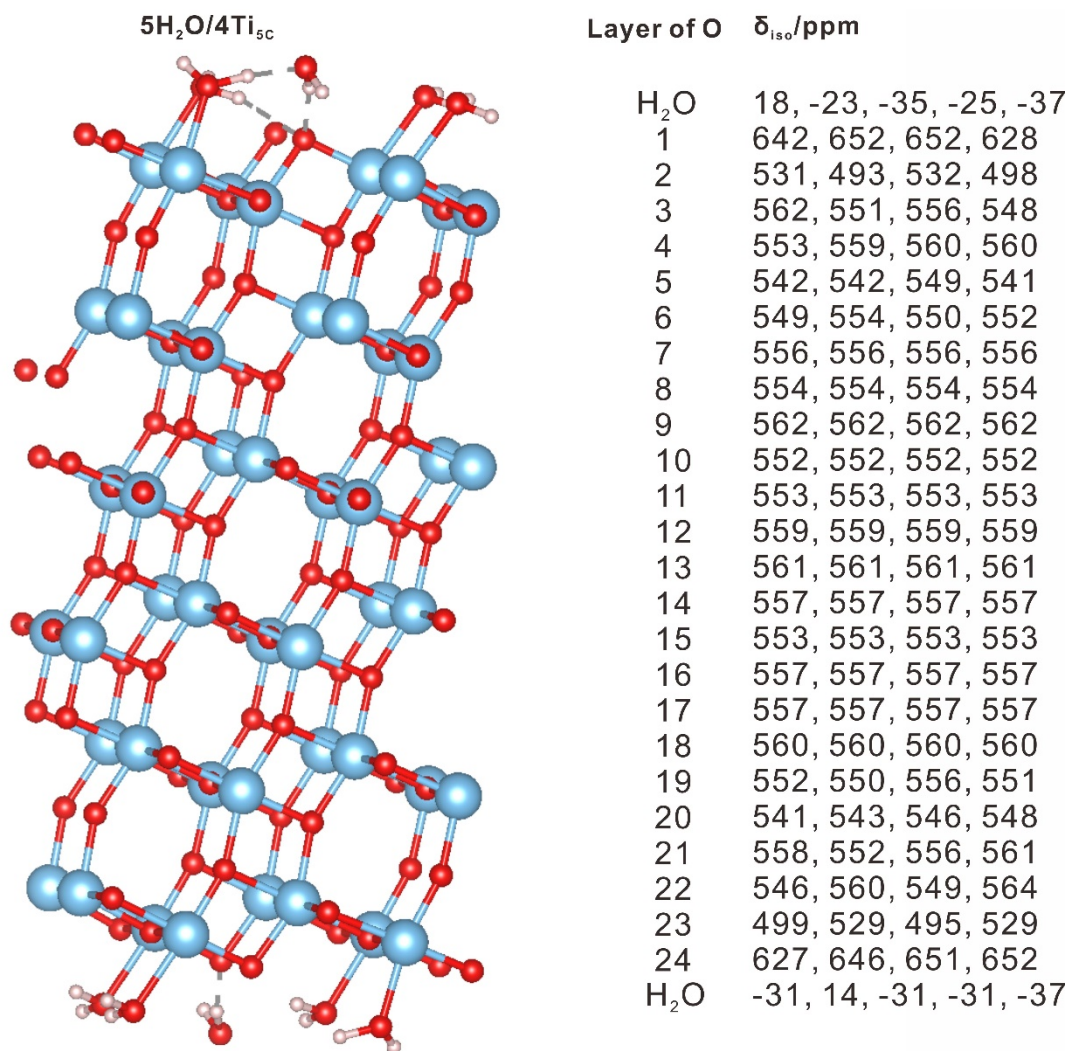
4H₂O/2Ti₅c

Layer of O	δ_{iso}/ppm
H₂O	18, -22
1	682, 692
2	507, 513
3	532, 533
4	551, 541
5	546, 549
6	544, 543
7	553, 553
8	561, 561
9	555, 555
10	551, 551
11	551, 551
12	561, 561
13	555, 555
14	552, 552
15	550, 550
16	557, 557
17	551, 551
18	552, 552
19	544, 539
20	545, 554
21	540, 539
22	530, 528
23	506, 493
24	669, 746
H₂O	22, -36

Figure S19. Calculated structure of the TiO₂ (101) facet with adsorbed water molecules. In this model, two water molecules are chemisorbed on two surface Ti₅c sites and another two water molecules are physisorbed on the H₂O−Ti₅c through hydrogen bond. This structure is denoted as 4H₂O/2Ti₅c in the text. Isotropic chemical shifts δ_{iso} of the oxygen sites in each layer are listed, for which δ_{ref} = 130. Titanium, oxygen and hydrogen atoms are plotted in blue (Ti), red (O) and pink (H).

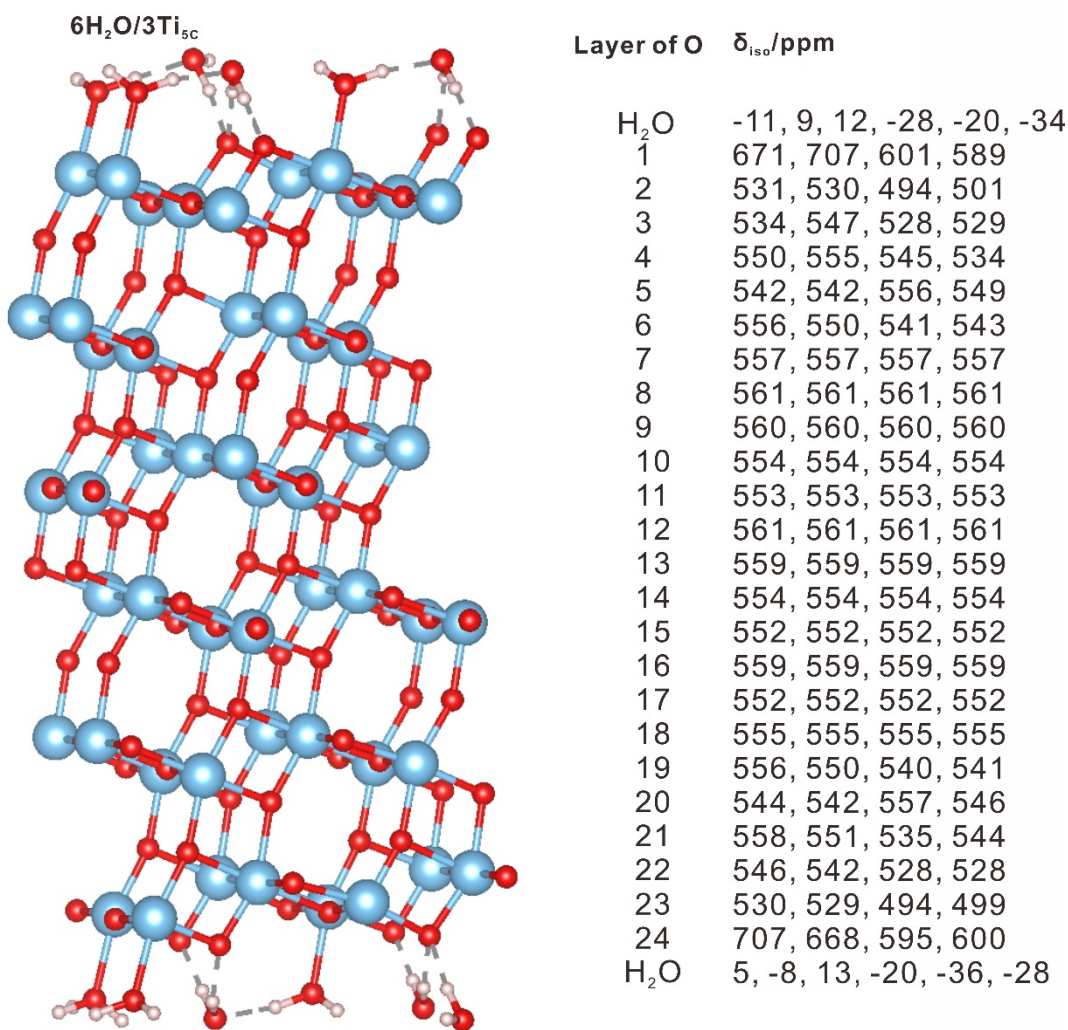**4H$_2$O/3Ti$_{5C}$**

Layer of O	δ_{iso}/ppm
H$_2$O	-33, 12, -39, -45
1	721, 730, 649, 628
2	529, 526, 484, 493
3	554, 560, 546, 536
4	555, 565, 558, 539
5	536, 555, 556, 552
6	555, 555, 547, 544
7	561, 556, 556, 560
8	561, 561, 561, 561
9	560, 560, 560, 560
10	557, 557, 557, 557
11	556, 556, 556, 556
12	561, 561, 561, 559
13	558, 558, 558, 558
14	557, 557, 557, 557
15	557, 557, 557, 557
16	561, 561, 561, 561
17	552, 552, 552, 552
18	557, 557, 557, 557
19	557, 554, 547, 545
20	542, 547, 556, 550
21	565, 556, 539, 559
22	560, 554, 537, 545
23	526, 527, 484, 492
24	733, 725, 660, 615
H$_2$O	8, -40, -38, -46

Figure S20. Calculated structure of the TiO$_2$ (101) facet with adsorbed water molecules. In this model, three water molecules are chemisorbed on three surface Ti$_{5C}$ sites and another water molecule is physisorbed on the H$_2$O−Ti$_{5C}$ through hydrogen bond. This structure is denoted as 4H$_2$O/3Ti$_{5C}$ in the text. Isotropic chemical shifts δ_{iso} of the oxygen sites in each layer are listed, for which δ_{ref} = 133. Titanium, oxygen and hydrogen atoms are plotted in blue (Ti), red (O) and pink (H).
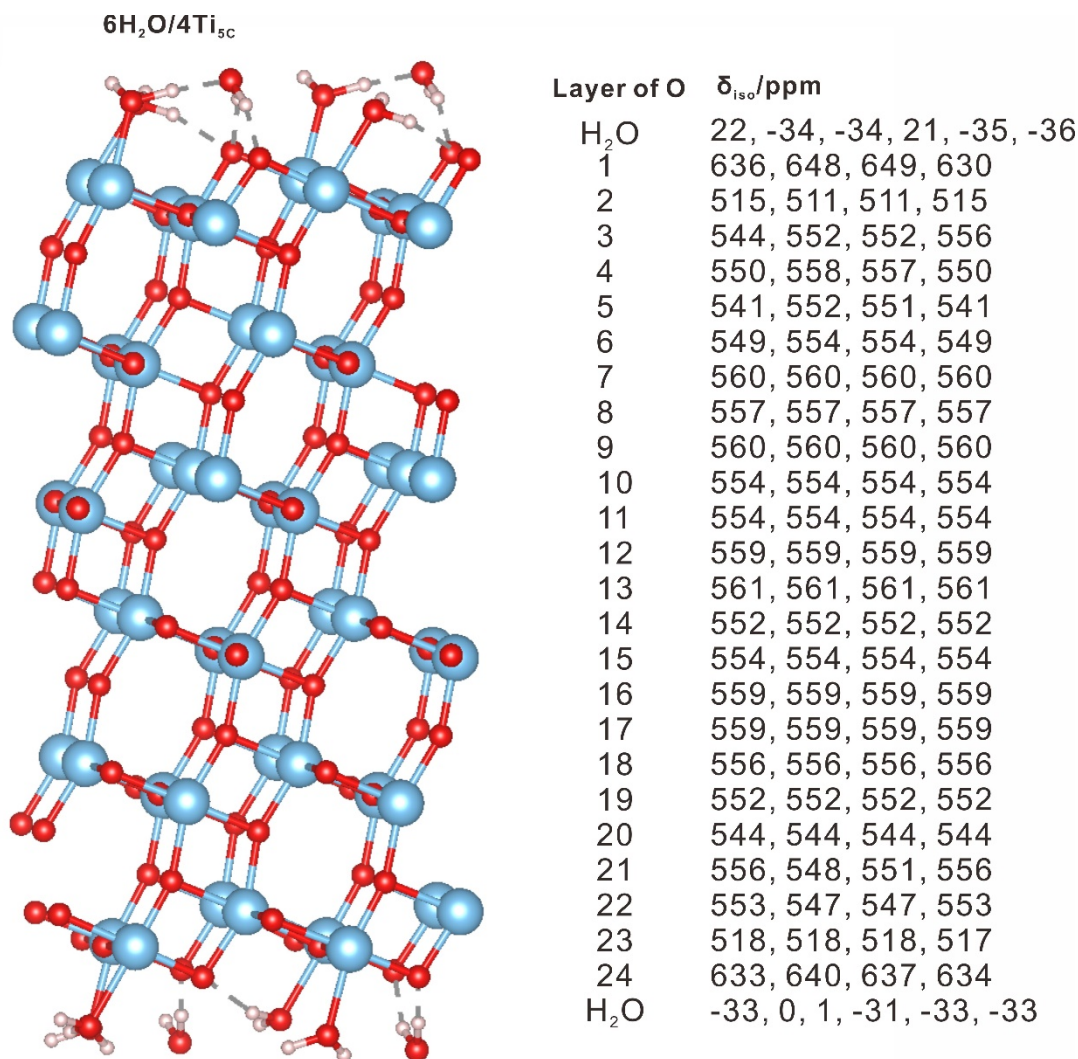
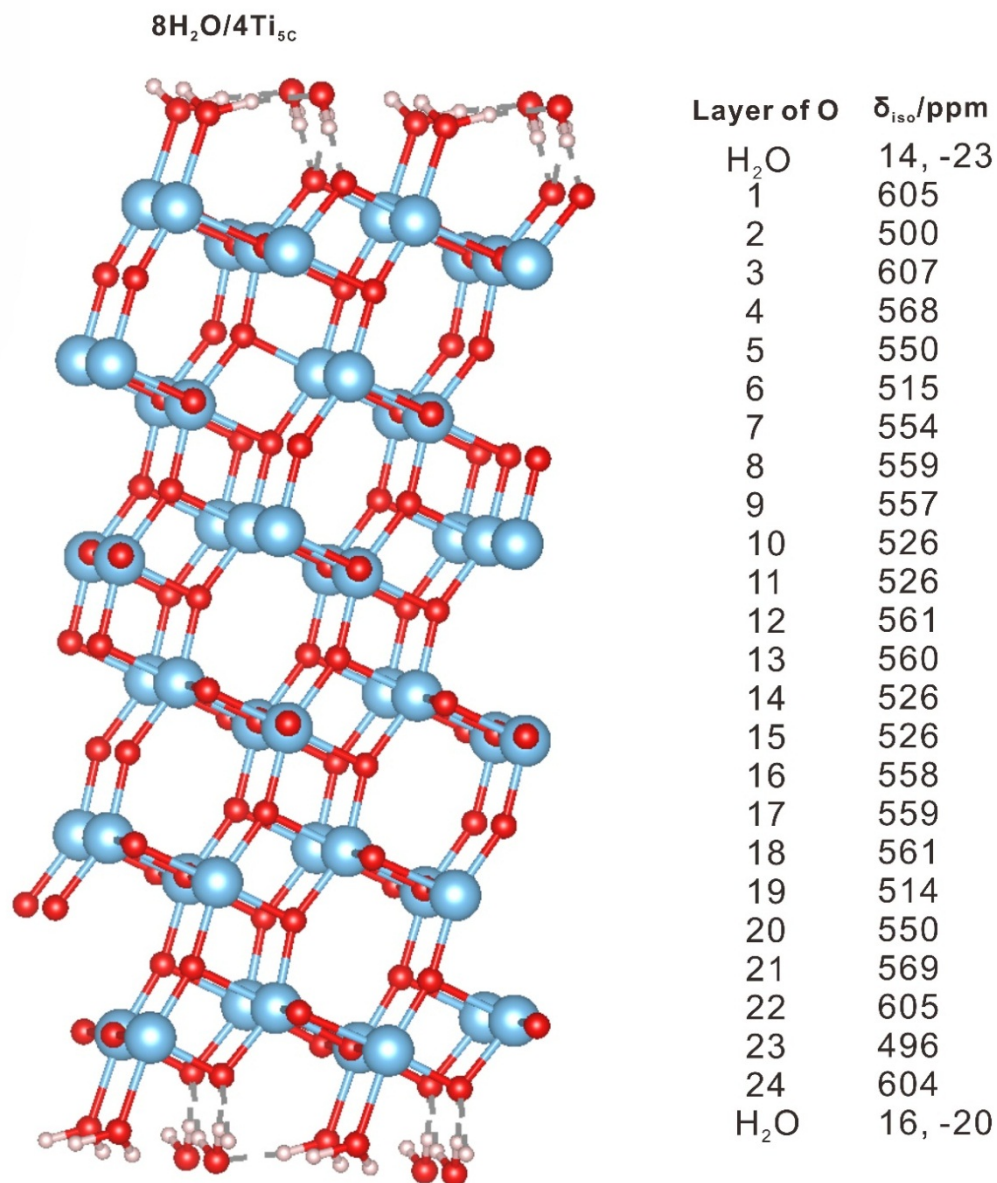| 5H$_2$O/4Ti$_{5C}$	Layer of O	δ_{iso}/ppm
	H$_2$O	18, -23, -35, -25, -37
	1	642, 652, 652, 628
	2	531, 493, 532, 498
	3	562, 551, 556, 548
	4	553, 559, 560, 560
	5	542, 542, 549, 541
	6	549, 554, 550, 552
	7	556, 556, 556, 556
	8	554, 554, 554, 554
	9	562, 562, 562, 562
	10	552, 552, 552, 552
	11	553, 553, 553, 553
	12	559, 559, 559, 559
	13	561, 561, 561, 561
	14	557, 557, 557, 557
	15	553, 553, 553, 553
	16	557, 557, 557, 557
	17	557, 557, 557, 557
	18	560, 560, 560, 560
	19	552, 550, 556, 551
	20	541, 543, 546, 548
	21	558, 552, 556, 561
	22	546, 560, 549, 564
	23	499, 529, 495, 529
	24	627, 646, 651, 652
	H$_2$O	-31, 14, -31, -31, -37

Figure S21. Calculated structure of the TiO$_2$ (101) facet with adsorbed water molecules. In this model, four water molecules are chemisorbed on four surface Ti$_{5C}$ sites and another one water molecule is physisorbed on the H$_2$O−Ti$_{5C}$ through hydrogen bond. This structure is denoted as 5H$_2$O/4Ti$_{5C}$ in the text. Isotropic chemical shifts δ_{iso} of the oxygen sites in each layer are listed, for which δ_{ref} = 131. Titanium, oxygen and hydrogen atoms are plotted in blue (Ti), red (O) and pink (H).

**6H$_2$O/3Ti$_{5C}$**

Layer of O	δ_{iso}/ppm
H$_2$O	-11, 9, 12, -28, -20, -34
1	671, 707, 601, 589
2	531, 530, 494, 501
3	534, 547, 528, 529
4	550, 555, 545, 534
5	542, 542, 556, 549
6	556, 550, 541, 543
7	557, 557, 557, 557
8	561, 561, 561, 561
9	560, 560, 560, 560
10	554, 554, 554, 554
11	553, 553, 553, 553
12	561, 561, 561, 561
13	559, 559, 559, 559
14	554, 554, 554, 554
15	552, 552, 552, 552
16	559, 559, 559, 559
17	552, 552, 552, 552
18	555, 555, 555, 555
19	556, 550, 540, 541
20	544, 542, 557, 546
21	558, 551, 535, 544
22	546, 542, 528, 528
23	530, 529, 494, 499
24	707, 668, 595, 600
H$_2$O	5, -8, 13, -20, -36, -28

Figure S22. Calculated structure of the TiO$_2$ (101) facet with adsorbed water molecules. In this model, three water molecules are chemisorbed on three surface Ti$_{5C}$ sites and another three water molecules are physisorbed on the H$_2$O−Ti$_{5C}$ through hydrogen bond. This structure is denoted as 6H$_2$O/3Ti$_{5C}$ in the text. Isotropic chemical shifts δ_{iso} of the oxygen sites in each layer are listed, for which δ_{ref} = 130. Titanium, oxygen and hydrogen atoms are plotted in blue (Ti), red (O) and pink (H).

6H$_2$O/4Ti$_{5C}$

Layer of O	δ_{iso}/ppm
H$_2$O	22, -34, -34, 21, -35, -36
1	636, 648, 649, 630
2	515, 511, 511, 515
3	544, 552, 552, 556
4	550, 558, 557, 550
5	541, 552, 551, 541
6	549, 554, 554, 549
7	560, 560, 560, 560
8	557, 557, 557, 557
9	560, 560, 560, 560
10	554, 554, 554, 554
11	554, 554, 554, 554
12	559, 559, 559, 559
13	561, 561, 561, 561
14	552, 552, 552, 552
15	554, 554, 554, 554
16	559, 559, 559, 559
17	559, 559, 559, 559
18	556, 556, 556, 556
19	552, 552, 552, 552
20	544, 544, 544, 544
21	556, 548, 551, 556
22	553, 547, 547, 553
23	518, 518, 518, 517
24	633, 640, 637, 634
H$_2$O	-33, 0, 1, -31, -33, -33

Figure S23. Calculated structure of the TiO$_2$ (101) facet with adsorbed water molecules. In this model, four water molecules are chemisorbed on four surface Ti$_{5C}$ sites and another two water molecules are physisorbed on the H$_2$O−Ti$_{5C}$ through hydrogen bond. This structure is denoted as 6H$_2$O/4Ti$_{5C}$ in the text. Isotropic chemical shifts δ_{iso} of the oxygen sites in each layer are listed, for which δ_{ref} = 132. Titanium, oxygen and hydrogen atoms are plotted in blue (Ti), red (O) and pink (H).

8H₂O/4Ti₅C

Layer of O	δ_{iso}/ppm
H_2O	14, -23
1	605
2	500
3	607
4	568
5	550
6	515
7	554
8	559
9	557
10	526
11	526
12	561
13	560
14	526
15	526
16	558
17	559
18	561
19	514
20	550
21	569
22	605
23	496
24	604
H_2O	16, -20

Figure S24. Calculated structure of the TiO_2 (101) facet with adsorbed water molecules. In this model, four water molecules are chemisorbed on four surface Ti_{5C} sites and another four water molecules are physisorbed on the $H_2O−Ti_{5C}$ through hydrogen bond. This structure is denoted as $8H_2O/4Ti_{5C}$ in the text. Isotropic chemical shifts δ_{iso} of the oxygen sites in each layer are listed, for which δ_{ref} = 166. Titanium, oxygen and hydrogen atoms are plotted in blue (Ti), red (O) and pink (H).
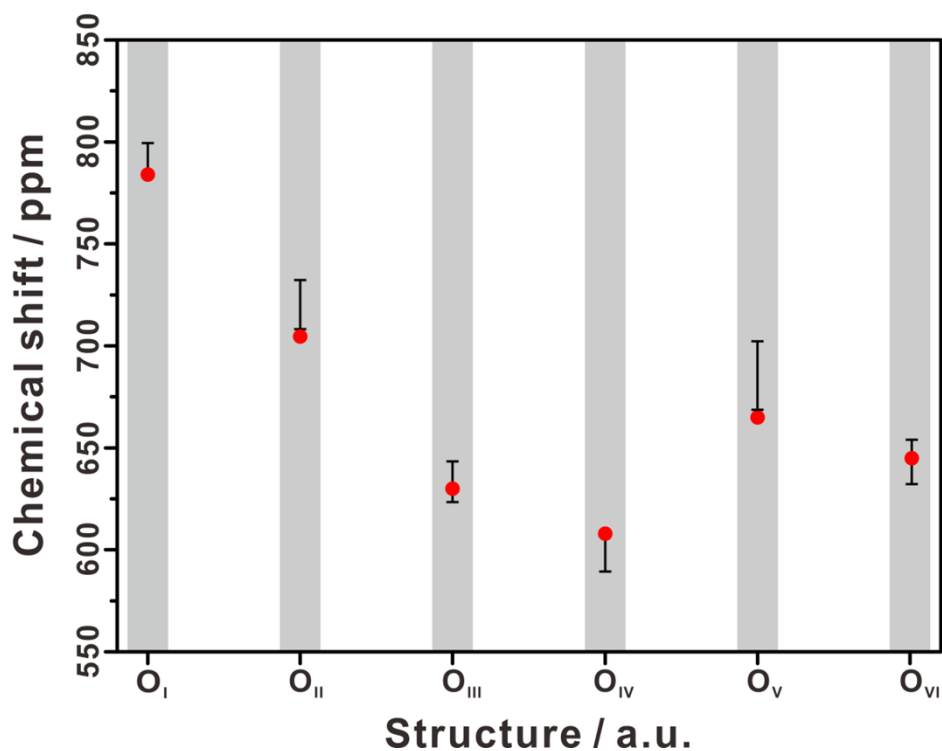
Figure S25. Calculated ^{17}O chemical shifts of various O_{2C} sites interacting with H_2O on (101) facet of TiO_2 (Bar), and the corresponding NMR experimental values (Red dot). According to our NMR results, two types of adsorbed H_2O (chemisorbed H_2O, i.e. $Ti_{5C}-OH_2$ and physisorbed H_2O) are present on the (101) facet of TiO_2, and the formation of $O_{II}-O_{VI}$ sites is associated with the interaction between O_I (the bare O_{2C} site) and adsorbed H_2O. Thus, a series of structures with different H_2O adsorption configuration on (2 × 2) TiO_2 (101) surface slabs are optimized and shown in Figures S12−S24. Theoretical calculations indicate that the two types of adsorbed H_2O can form hydrogen bonds with nearby O_{2C} sites. Six O_{2C} sites having interaction with H_2O in different adsorption configuration are summarized from the calculated structures on (2 × 2) surface slabs (Figure 3b in main text). Based on our theoretically calculated and experimental ^{17}O NMR chemical shifts (Figure S25), as well as the evolution of surface O_{2C} sites with the increase of H_2O loading (Figure 3a in main text), the following assignments can be made: O_I is due to surface O_{2C} site without interaction with H_2O; O_{II} and O_{III} correspond to surface O_{2C} sites interacting with one and two chemisorbed H_2O, respectively; O_{IV} is assigned to surface O_{2C} site interacting with two chemisorbed H_2O and two physisorbed H_2O; O_V is attributed to surface O_{2C} site interacting with one chemisorbed H_2O and one physisorbed H_2O; O_{VI} is due to surface O_{2C} site interacting with two chemisorbed H_2O and one physisorbed H_2O.
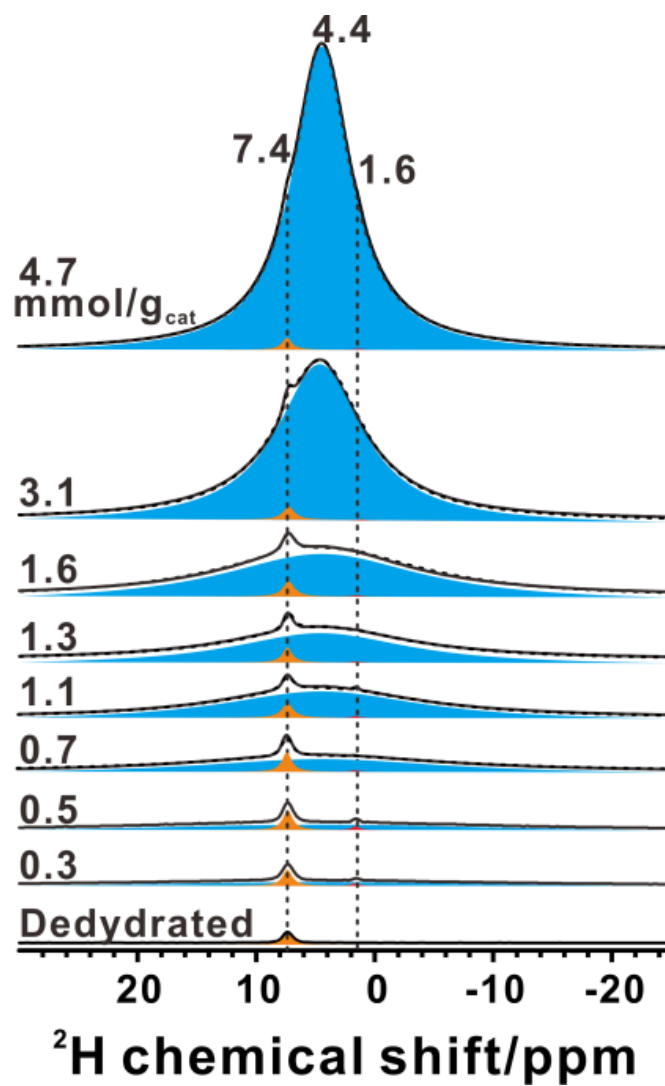
Figure S26. Experimental and simulated ^2H MAS NMR spectra of dehydrated ^2H-enriched TiO_2 samples with ^2H_2O loading from 0 to 4.7 mmol/g.
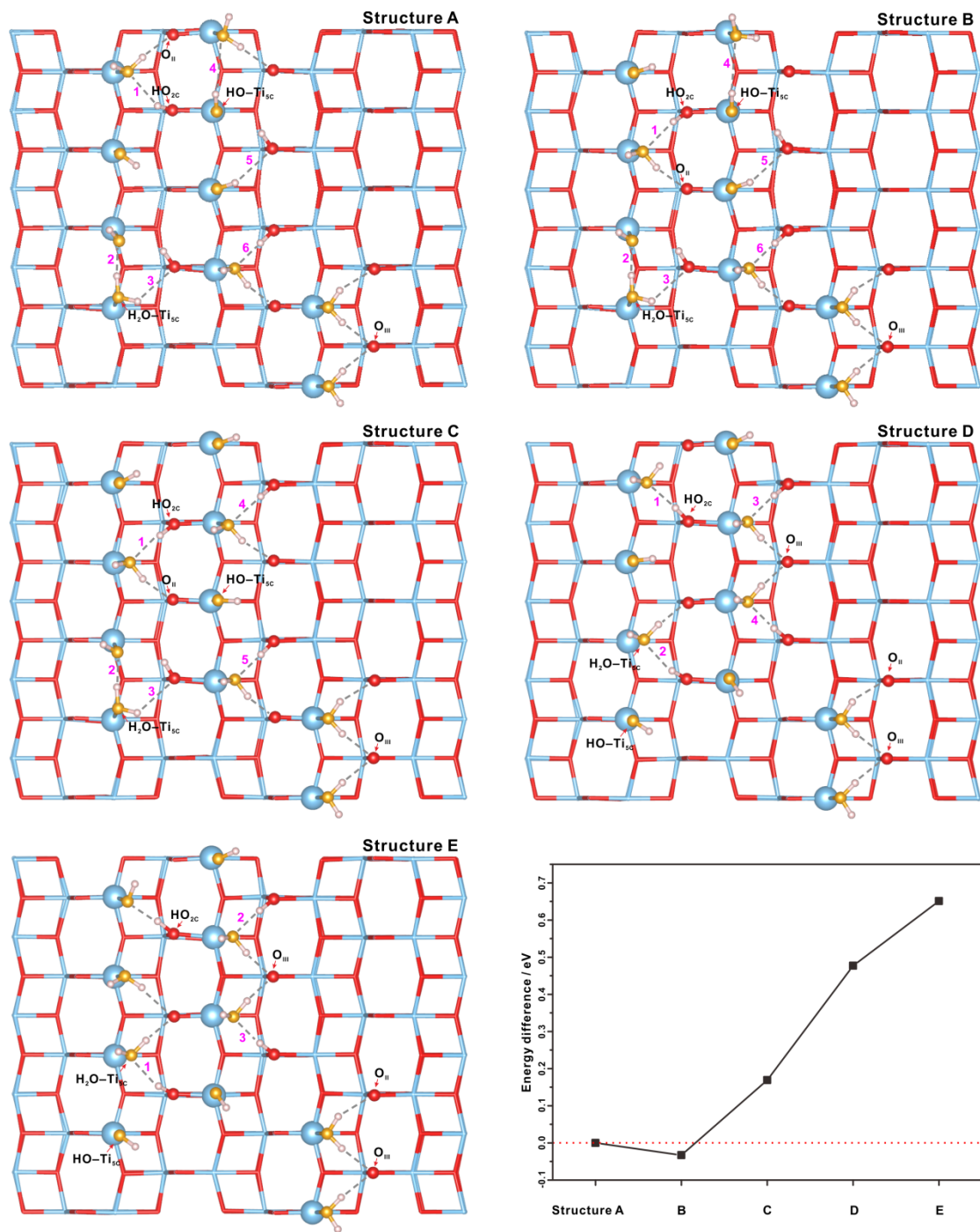
Figure S27. The optimized dissociation states of the interfacial H_2O on the (101) facet of TiO_2 at a 40% coverage with different amount of OH – H_2O interaction in the form of M_I – M_{VI} conformations (Figure 2 in main text), and the energy difference of the different OH / H_2O configurations (Structure A with six OH – H_2O interactions, Structure B with six OH – H_2O interactions, Structure C with five OH – H_2O interactions, Structure D with four OH – H_2O interactions, and Structure E with three OH – H_2O interactions). To verify the interactions between OH and

H_2O on anatase TiO_2 (101) surface, we performed structure optimization of five geometries with OH species (including $Ti_{5C}-OH$ and $O_{2C}H$) and H_2O molecules on TiO_2 (101) surface. The calculations were performed by using a large (5×5×1) supercell slab (a=b=27.21 Å) with 300 atoms (100 Ti atoms and 200 O atoms) containing a vacuum gap of 15 Å. With such a big supercell, we use gamma point only to sample the surface Brillouin zone. The OH species and H_2O molecules were put on one side of the supercell and the atoms in the most bottom layer atoms were fixed during the calculations. With the increase of the OH – H_2O interactions, the energy of the OH/H_2O configurations decrease gradually, indicating that the OH – H_2O interactions can stabilize the dissociation of H_2O, and hinder the reaction of bridging OH groups and adjacent terminal OH groups to regenerate molecular H_2O.
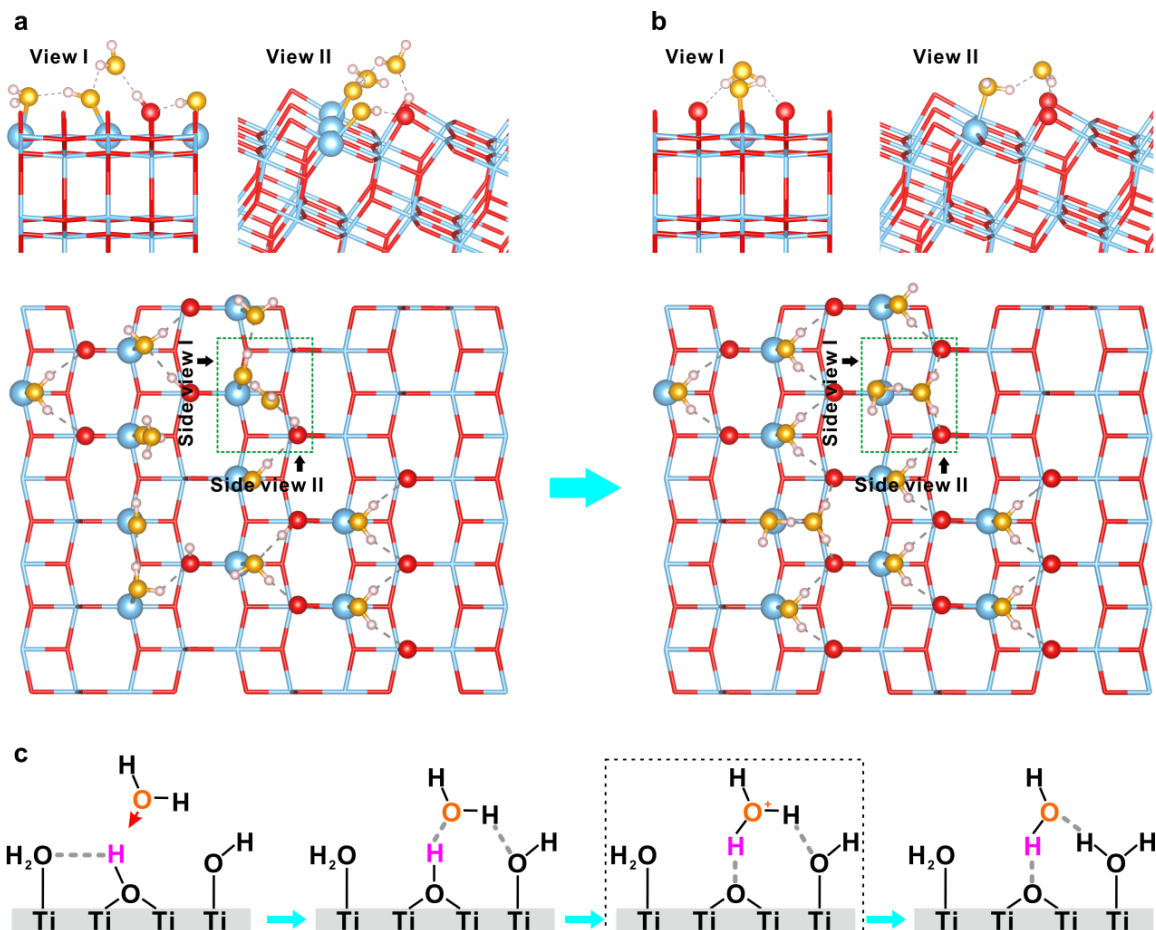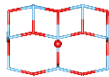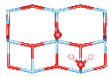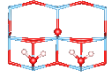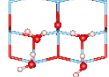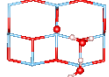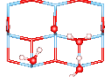
Figure S28. (a) The dissociation state of interfacial H_2O on the (101) facet of TiO_2 at a 65% coverage of water. In this model, the physisorbed H_2O is shown in the green square. (b) The molecular H_2O adsorbed on the (101) facet of TiO_2 at the 65% coverage of water. (c) Scheme of regenerating H_2O via the interaction between two OH groups originated from H_2O dissociation. According to the ^{2}H MAS NMR results (Figure 4 in main text), the proton of bridging OH group is active and can exchange with ^{2}H of D_2O. As such, when the physisorbed H_2O is adsorbed on the proton of bridged OH group through hydrogen bond, its original interaction with chemisorbed H_2O is broken, and an H_3O^+-like transition state could be formed as revealed in the previous report [11], which can react with adjacent terminal OH group to re-generate H_2O.

Table S1. ^{17}O NMR parameters for oxygen sites on TiO$_2$ (101) surface.

O sites	Experimental results		Calculated structures
	δ_{iso}/ppm	P$_Q$/MHz	
O$_I$	785[a]	8.2[a]	
O$_{II}$	702	0.9	
O$_{III}$	628	0.0	
O$_{IV}$	615	0.0	
O$_V$	658	0.4	
O$_{VI}$	641	0.7	

Isotropic chemical shifts (δ_{iso}) and quadrupolar parameters (P$_Q$) are derived from the 2D ^{17}O 3Q MAS spectra in Figure 1d and 1E. $\delta_{iso} = \frac{17}{27}\delta_{F1} + \frac{10}{27}\delta_{F2}$;
$P_Q = v_0 \sqrt{\frac{17}{675000}(\delta_{F1} - \delta_{F2})} = C_Q \times \sqrt{\frac{\eta^2}{3} + 1}$, where v_0 is resonance frequency of oxygen nucleus the η is the asymmetric parameter of the electric field gradient (EFG) tensor.

[a] Extracted by fitting the 1D ^{17}O MAS spectra in Figure 1c using the Dimfit program. The C$_Q$ and η of O$_I$ is 8.0 MHz and 0.38, respectively.

Table S2. Theoretical calculated adsorption energy of H_2O on TiO_2 with different H_2O adsorption. $\Delta E = E(M) - [E(Bare\text{-}TiO_2) + n \times E(H_2O)]$, where ΔE is the adsorption energy of H_2O, $E(M)$ is the total energy of the adsorption complex, $E(Bare\text{-}TiO_2) = -1266.6306$ eV, $E(H_2O) = -14.209828$ eV, and n is the number of adsorbed H_2O.

$1H_2O/TiO_2$	**$1H_2O/1Ti_{5C}$**		
	ΔE=-15.56 eV		
$2H_2O/TiO_2$	**$2H_2O/1Ti_{5C}$**	**$2H_2O/2Ti_{5C}$**	
	ΔE=-30.93eV	**ΔE=-31.59eV**	
$3H_2O/TiO_2$	**$3H_2O/2Ti_{5C}$**	**$3H_2O/3Ti_{5C}$**	
	ΔE=-46.73eV	**ΔE=-46.82eV**	
$4H_2O/TiO_2$	**$4H_2O/2Ti_{5C}$**	**$4H_2O/3Ti_{5C}$**	**$4H_2O/4Ti_{5C}$**
	ΔE=-62.33eV	**ΔE=-62.39eV**	**ΔE=-62.78eV**
$5H_2O/TiO_2$	**$5H_2O/4Ti_{5C}$**		
	ΔE=-77.86eV		
$6H_2O/TiO_2$	**$6H_2O/3Ti_{5C}$**	**$6H_2O/4Ti_{5C}$**	
	ΔE=-93.22eV	**ΔE=-93.44eV**	
$8H_2O/TiO_2$	**$8H_2O/4Ti_{5C}$**		
	ΔE=-122.37eV		

Note 1: nH_2O/TiO_2 represents n H_2O molecules adsorbed on TiO_2 surface.
Note 2: nH_2O/mTi_{5C} (n≥m) represents m H_2O molecules chemisorbed on m Ti_{5C} sites ($Ti_{5C}-OH_2$) of (2 × 2) surface slabs and (n-m) H_2O molecules physisorbed on (n-m) $Ti_{5C}-OH_2$.

Table S3. The structural parameters (bond length and bond angle) of interfacial H_2O and TiO_2 framework for the (2 × 2) TiO_2 (101) surface slabs with variable H_2O adsorption.

1H₂O/1Ti₅c

H₂O-I

D1/Å	D2/Å	A1/°	A2/°
0.986	1.914	103.17	98.78

2H₂O/2Ti₅c

H₂O-I

D1/Å	D2/Å	A1/°	A2/°
0.985	1.913	103.15	100.84

H₂O-II

D1/Å	D2/Å	A1/°	A2/°
0.985	1.913	103.15	100.84

3H₂O/3Ti₅c
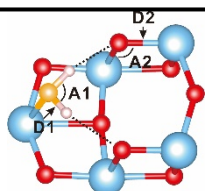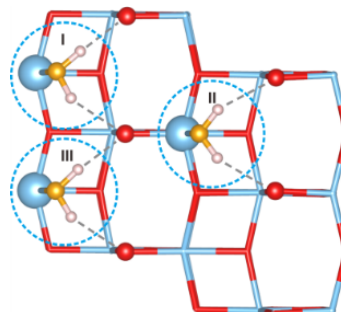
	D1/Å	D2/Å	A1/°	A2/°
H₂O-I	0.983	1.910	103.51	101.13
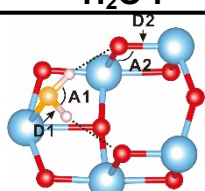
	D1/Å	D2/Å	A1/°	A2/°
H₂O-II	0.993	1.965	101.92	99.55
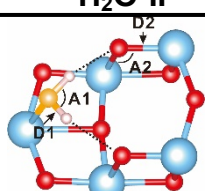
	D1/Å	D2/Å	A1/°	A2/°
H₂O-III	0.991	1.965	101.84	99.55

4H₂O/4Ti₅c
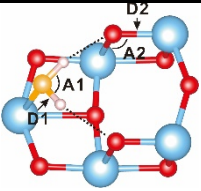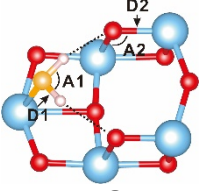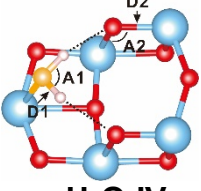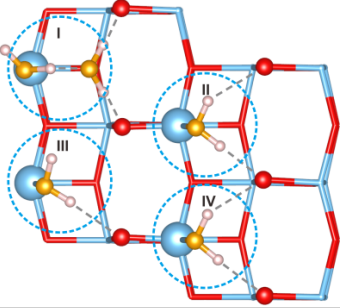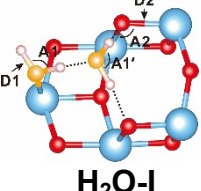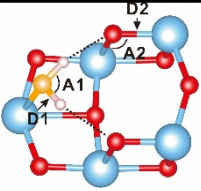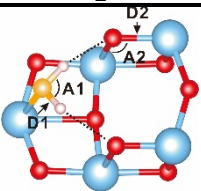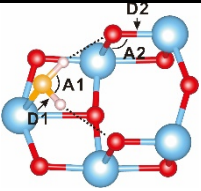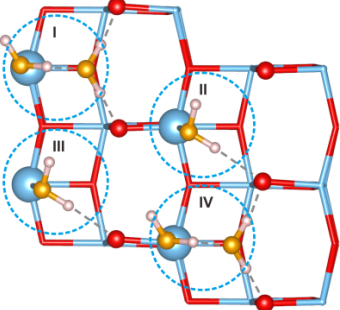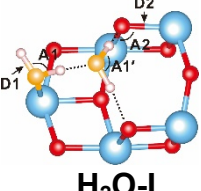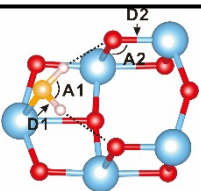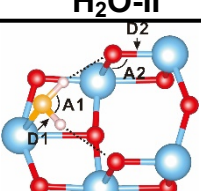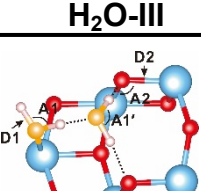
	D1/Å	D2/Å	A1/°	A2/°
H₂O-I	0.983	2.053	101.12	98.68

	D1/Å	D2/Å	A1/°	A2/°
H₂O-II	0.983	2.053	101.12	98.68

	D1/Å	D2/Å	A1/°	A2/°
H₂O-III	0.983	2.053	101.12	98.68

	D1/Å	D2/Å	A1/°	A2/°
H₂O-IV	0.983	2.053	101.12	98.68

$5H_2O/4Ti_5c$

	D1/Å	D2/Å	A1/°	A1'/°	A2/°
H₂O-I	1.045	1.938	107.95	102.80	100.57

	D1/Å	D2/Å	A1/°	A2/°
H₂O-II	0.996	1.937	102.55	99.63

	D1/Å	D2/Å	A1/°	A2/°
H₂O-III	0.989	1.938	104.51	100.57

	D1/Å	D2/Å	A1/°	A2/°
H$_2$O-IV	0.991	1.937	102.66	99.63

6H$_2$O/4Ti$_5$c

	D1/Å	D2/Å	A1/°	A1'/°	A2/°
H$_2$O-I	1.049	1.934	102.75	102.72	99.44

	D1/Å	D2/Å	A1/°	A2/°
H$_2$O-II	0.994	1.934	104.70	99.44

	D1/Å	D2/Å	A1/°	A2/°
H$_2$O-III	0.994	1.934	104.70	99.44

	D1/Å	D2/Å	A1/°	A1'/°	A2/°
H$_2$O-IV	1.049	1.934	102.75	102.72	99.44

8H₂O/4Ti₅c
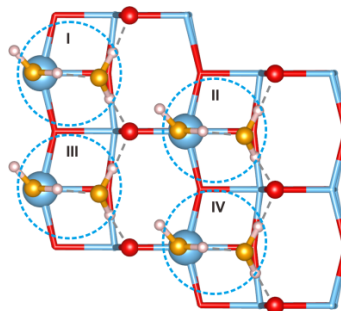
	D1/Å	D2/Å	A1/°	A1'/°	A2/°
H₂O-I	1.022	1.971	107.82	101.71	101.69
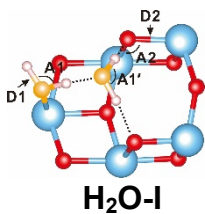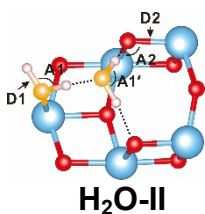
	D1/Å	D2/Å	A1/°	A1'/°	A2/°
H₂O-II	1.022	1.971	107.82	101.71	101.69

	D1/Å	D2/Å	A1/°	A1'/°	A2/°
H₂O-III	1.022	1.971	107.82	101.71	101.69
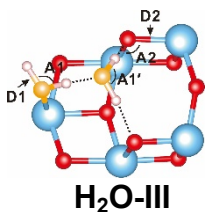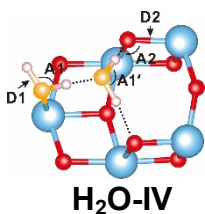
	D1/Å	D2/Å	A1/°	A1'/°	A2/°
H₂O-IV	1.022	1.971	107.82	101.71	101.69

Table S4. ^{2}H NMR parameters for chemisorbed D_2O on TiO_2 (101) surface. Isotropic chemical shifts (δ_{iso}) and quadrupolar parameters (C_Q and η) are extracted by spectral fitting of variable-temperature static ^{2}H NMR spectra using the Dimfit program.

Temperature/K	δ_{iso}/ppm	C_Q/kHz	η
150	4.8	209	0.1
180	4.8	205	0.1
200	4.8	190	0.1
220	4.8	150	0.1

SI References

1   L. Liu, X. Gu, Z. Ji, W. Zou, C. Tang, F. Gao and L. Dong, Anion-Assisted Synthesis of TiO_2 Nanocrystals with Tunable Crystal Forms and Crystal Facets and Their Photocatalytic Redox Activities in Organic Reactions, *J. Phys. Chem. C*, 2013, **117**, 18578−18587.

2   A. Jia, Y. Zhang, T. Song, Z. Zhang, C. Tang, Y. Hu, W. Zheng, M. Luo, J. Lu and W. Huang, Crystal-plane effects of anatase TiO_2 on the selective hydrogenation of crotonaldehyde over Ir/TiO_2 catalysts, *J. Catal.*, 2021, **395**, 10−22.

3   G. Kresse and J. Furthmüller, Efficiency of ab-initio total energy calculations for metals and semiconductors using a plane-wave basis set, *Comp. Mater. Sci.*, 1996, **6**, 15−50.

4   J. P. Perdew, K. Burke and M. Ernzerhof, Generalized gradient approximation made simple, *Phys. Rev. Lett.*, 1996, **77**, 3865−3868.

5   Y. Li, X.-P. Wu, N. Jiang, M. Lin, L. Shen, H. Sun, Y. Wang, M. Wang, X. Ke, Z. Yu, F. Gao, L. Dong, X. Guo, W. Hou, W. Ding, X.-Q. Gong, C. P. Grey and L. Peng, Distinguishing Faceted Oxide Nanocrystals with ^{17}O Solid-State NMR Spectroscopy, *Nat. Commun.*, 2017, **8**, 581.

6   J. K. Burdett, T. Hughbanks, G. J. Miller, J. W. Richardson and J. V. Smith, Structural-electronic relationships in inorganic solids: powder neutron diffraction studies of the rutile and anatase polymorphs of titanium dioxide at 15 and 295 K, *J. Am. Chem. Soc.*, 1987, **109**, 3639−3646.

7   D. J. Chadi, Special points for Brillouin-zone integrations, *Phys. Rev. B*, 1977, **16**, 1746−1747.

8   J. Yu, J. Low, W. Xiao, P. Zhou and M. Jaroniec, Enhanced photocatalytic CO_2-reduction activity of anatase TiO_2 by co-exposed {001} and {101} facets, *J. Am. Chem. Soc.*, 2014, **136**, 8839-8842.

9   C. Xu, W. Yang, Q. Guo, D. Dai, M. Chen and X. Yang, Molecular hydrogen formation from photocatalysis of methanol on anatase-TiO$_2$(101), *J. Am. Chem. Soc.*, 2014, **136**, 602-605.

10 Q. Han, C. Wu, H. Jiao, R. Xu, Y. Wang, J. Xie, Q. Guo and J. Tang, Rational design of high-concentration Ti^{3+} in porous carbon-doped TiO$_2$ nanosheets for efficient photocatalytic ammonia synthesis, *Adv. Mater.*, 2021, **33**, e2008180.

11   L. R. Merte, G. Peng, R. Bechstein, F. Rieboldt, C. A. Farberow, L. C. Grabow, W. Kudernatsch, S. Wendt, E. Lægsgaard, M. Mavrikakis and F. Besenbacher, Water-Mediated Proton Hopping on an Iron Oxide Surface, *Science*, 2012, **336**, 889−893.